Archboldomys (Muridae: Murinae) Reconsidered: A New Genus and Three New Species of Shrew Mice from Luzon Island, Philippines

DANILO S. BALETE,[1] ERIC A. RICKART,[2] LAWRENCE R. HEANEY,[1]
PHILLIP A. ALVIOLA,[3] MELIZAR V. DUYA,[4] MARIANO ROY M. DUYA,[4]
TIMOTHY SOSA,[1,5] AND SHARON A. JANSA[5]

ABSTRACT

Shrew mice of the genus *Archboldomys* are poorly known members of an endemic clade of vermivorous/insectivorous murid rodents confined to Luzon Island, Philippines. Three species of these small, ground-living, diurnal mice were previously known, all from a handful of specimens from a few localities. The pattern of morphological and genetic differentiation among additional specimens of shrew mice from our recent field surveys in the Central Cordillera and Sierra Madre mountains of Luzon document the presence of two distinct species groups within *Archboldomys* as previously defined, as well as three new species. Gene-sequence data from the mitochondrial cytochrome *b* and nuclear IRBP genes confirm the existence of six distinct species, but also show that *Archboldomys*, as previously defined, is composed of two clades that are not sister taxa. Reevaluation of the presumed morphological synapomorphies among these shrew mice, together with analyses of karyological and gene-sequence data, support the following: (1) erection of *Soricomys*, new genus; (2) transfer of *A. kalinga* and *A. musseri* to *Soricomys;* and (3) recognition of *Archboldomys maximus*,

[1] Field Museum of Natural History, 1400 S. Lake Shore Drive, Chicago, IL 60605.
[2] Utah Museum of Natural History, University of Utah, 301 Wakara Way, Salt Lake City, Utah 84108.
[3] Museum of Natural History, University of the Philippines at Los Banos, College, Laguna 4031, Philippines.
[4] Conservation International, 6 Maalalahanin St., Teachers Village, Diliman, Quezon City 1101, Philippines; current address: Institute of Biology, University of the Philippines Diliman, Quezon City 1101, Philippines.
[5] Bell Museum of Natural History, University of Minnesota, Minneapolis, MN 55455.

n. sp., *Soricomys leonardocoi*, n. sp., and *Soricomys montanus,* n. sp. The new genus and species are described, and their phylogenetic relationships, biogeography, and conservation are discussed.

INTRODUCTION

Shrew mice of the genus *Archboldomys* are part of one of the oldest known radiations of murid rodents in the Philippines, and provide important insights into the dynamics of mammalian diversification on isolated oceanic islands (Jansa et al., 2006). Together with the shrew rats *Chrotomys* and *Rhynchomys*, their closest relatives, they form a clade of terrestrial murid rodents adapted to feeding on earthworms and soft-bodied invertebrates on the cool, damp forest floor of montane and mossy forest on the mountaintops of Luzon Island in the northern Philippines (Balete et al., 2011; Duya et al., 2011; Jansa et al., 2006; Rickart et al., 1991, 2011a). The sister taxon to these three genera is the genus *Apomys*, forest mice that also prefer soft-bodied invertebrates, but additionally feed on seeds and small fruits. These four genera form a clade that is endemic to the Philippines (referred to informally as the *Chrotomys* Division by Musser and Carleton, 2005, or as members of the Hydromyini within the Murinae by Aplin and Helgen, 2010; see also Jansa and Weksler, 2004; Rowe et al., 2008; Heaney et al., 2009), exhibiting spectacular ecological and morphological diversity, from small arboreal mice to ground-hopping, long-snouted, shrewlike rats. At least 45 species are currently known (Heaney et al., 2010, 2011).

Some members of this clade (e.g., *Chrotomys* and *Rhynchomys*) had previously confounded biologists, who speculated on the possible phylogenetic alliance(s) of this morphologically distinctive group. Based purely on morphological grounds, these Philippine endemics have been allied to Australo-Papuan murines in various subfamilial categories in the past, including Rhynchomyinae and Hydromyinae (Thomas, 1898; Ellerman, 1941; Simpson, 1945; Misonne, 1969). Among the members of this clade, the then monotypic genus *Archboldomys*, proved to be the most enigmatic. Since its description (Musser, 1982a) it was thought to be closely allied to *Crunomys*, another genus of shrewlike mice from the Philippines and Sulawesi (Musser, 1982a; Musser and Heaney, 1992). In 1998, the discovery of what was then considered another member of *Archboldomys* (*A. musseri* from Mt. Cetaceo, northeastern Luzon) and an additional new species of *Crunomys* (*C. suncoides* from Mindanao), together with karyotypic data from species of both genera, enabled a tentative reassessment of the inferred phylogenetic alliance between *Archboldomys* and *Crunomys* (Rickart et al., 1998). The results confirmed the phylogenetic link of *Archboldomys* with the *Chrotomys* Division, but found evidence that a close relationship with *Crunomys* was ambiguous, with possible convergence of the two on a shrewlike (i.e., Soricidae-like) morphology and trophic adaptation. This shrewlike morphology is associated with their heavy use of earthworms and other soft-bodied invertebrates captured in leaf litter (Rickart et al., 1991, 2011a; Heaney et al., 1999; Balete et al., 2011).

New characters and character states first evident in *A. musseri* and confirmed later in another new species, *A. kalinga*, were discussed within the context of broadening the morphological range of *Archboldomys* (Rickart et al., 1998; Balete et al., 2006). Subsequent DNA sequence data analyses supported the placement of *A. luzonensis* within the endemic *Chroto-*

mys Division of Philippine rodents, including *Apomys*, *Chrotomys*, and *Rhynchomys*; *Crunomys*, in contrast, was recovered as a sister taxon to *Maxomys*, within an entirely different clade of murines from the Philippines and the Sunda Shelf (Jansa et al., 2006).

Our additional fieldwork during 2006 to 2009 in the Central Cordillera and Mingan Mountains, both on Luzon Island (fig. 1), resulted in additional specimens of shrew mice from several locations (Rickart et al., 2011a, 2011b; Balete et al., 2011). Our analyses of their external, cranial, and dental features, together with additional karyological data from *A. kalinga*, and molecular sequence data from representatives of the *Chrotomys* Division, document the presence of three additional species of shrew mice described below. Unexpectedly, molecular sequence data has failed to support the monophyly of *Archboldomys*; although the two "species groups" are strongly supported as members of the *Chrotomys* Division, we find that *Archboldomys,* as currently defined, is paraphyletic and includes two divergent genera: *Archboldomys* and *Soricomys*, new genus, described below.

The above discoveries are consistent with and further strengthen the pattern revealed in previous studies in the Philippines (Esselstyn et al., 2009, 2011; Heaney et al., 2009, 2011; Jansa et al., 2006, 2009; Musser and Heaney, 1992; Steppan et al., 2003) and other large, geologically old oceanic islands (e.g., Madagascar: Olson and Goodman, 2003; Yoder et al., 1996) that their mammalian biodiversity arose from extensive in situ diversification. The discoveries reported here further illustrate the insularizing effect of isolated mountaintops in the Philippines on the diversification of its murid rodents (Balete et al., 2006, 2007, 2011; Heaney 1986; Heaney et al., 1989, 2009, 2011; Heaney and Rickart, 1990; Rickart et al., 1998, 2003, 2005; Steppan et al., 2003).

MATERIALS AND METHODS

Field and Preparation Procedures

The specimens examined in this study were all collected by the authors and their associates, except the holotype of *Archboldomys luzonensis*, which was collected by D.S. Rabor in 1961 (Musser, 1982a; Heaney et al., 1999; Rickart et al., 1991, 1998; Balete et al., 2006). These specimens are deposited at the Field Museum of Natural History (FMNH), the United States National Museum of Natural History, Smithsonian Institution (USNM), and the Philippine National Museum (PNM). The capture and handling of animals in the field followed all relevant laws and regulations of the Philippines.

Tissue samples were taken from the thigh muscle of fresh specimens and preserved in either 95% ethanol or DMSO buffer. Most of the specimens were injected with saturated formalin solution in the field, stored temporarily in 10% formalin, and subsequently transferred to 70% ethanol. Some skulls were then removed, cleaned with dermestid beetles, and briefly soaked in a weak ammonia solution. Some specimens were skeletonized in the field; these were cleaned in the same fashion as the skulls.

Reproductive data were taken in the field from skeletonized specimens or in the laboratory from autopsied specimens stored in 70% ethanol, including, for males: testes descent (scrotal or abdominal), testes size (length × width, in mm), and convolution of the epididymis; for females: number and position of mammae (inguinal, abdominal, axial), size and condition of
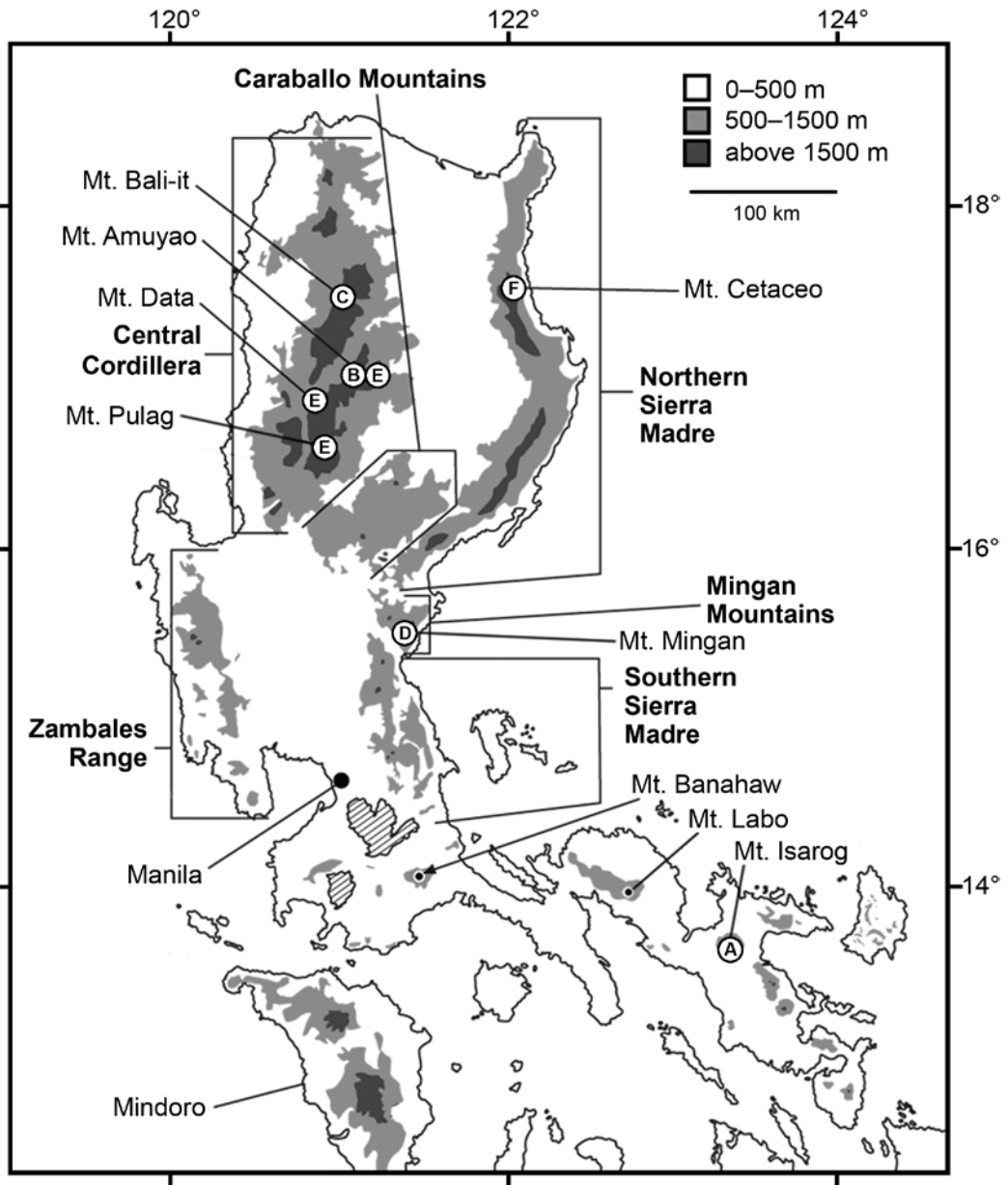
FIG. 1. Map of Luzon and adjacent islands. The major mountains and mountain ranges where *Archboldomys* and *Soricomys,* n. gen., occur are shown. One species, *A. luzonensis* (**A**) occurs on Mt. Isarog in the Bicol Peninsula of southern Luzon. Northern Luzon, where most of the high-elevation habitats occur, supports four species: *S. kalinga* (**C**) in the northern Central Cordillera, *S. leonardocoi*, n. sp. (**D**), in the Mingan Mountains, *A. maximus*, n. sp. (**B**) and *S. montanus*, n. sp. (**E**), in the southern Central Cordillera, and *S. musseri* (**F**) in the northern Sierra Madre.

mammae (small, large, lactating), presence or absence of vaginal perforation, number and size (crown to rump length, in mm) of embryos, and number of placental scars in the uterus.

Age determination was done in the field based on relative body size and reproductive condition of freshly caught specimens, and subsequently validated based on molar wear and fusion of cranial sutures, following the age categories defined by Musser and Heaney (1992). We followed the terminology of Brown (1971) and Brown and Yalden (1973) for defining the external features of the head and limbs. Terminology for cusps on molar teeth (fig. 2) and cranial foramina (fig. 3) was adapted from Musser and Heaney (1992: figs. 2, 8).
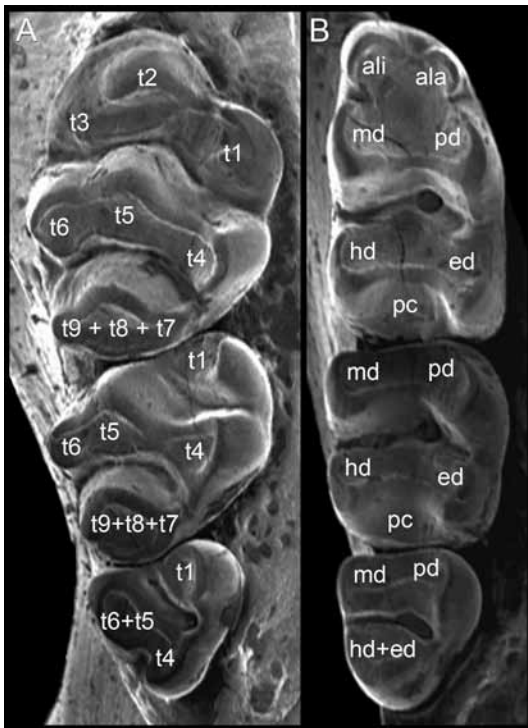
FIG. 2. Molar teeth of *Archboldomys maximus*, n. sp. (FMNH 193531, holotype), illustrating terminology used to describe cuspidation. Upper molars (left): cusps are numbered and referred to in the text with the prefix "t"; see Musser and Heaney, 1992. Lower molars (right): **ala**, anterolabial cusp; **ali**, anterolingual cusp; **ed**, entoconid; **hd**, hypoconid; **md**, metaconid; **pc**, posterior cingulum; **pd**, protoconid
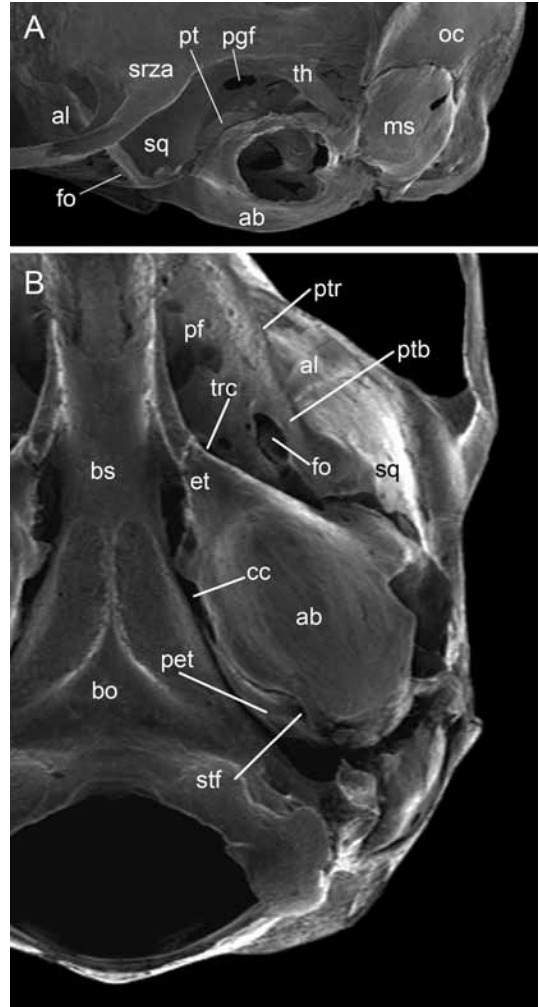

FIG. 3. Lateral and ventral views of the cranium of *Archboldomys maximus*, n. sp. (FMNH 193531, holotype), showing morphological features discussed in the text. Abbreviations: **ab**, auditory bulla; **al**, alisphenoid; **bo**, basioccipital; **bs**, basisphenoid; **cc**, carotid canal; **et**, eustachian tube; **fo**, foramen ovale; **ms**, mastoid; **pet**, petrosal portion of the petromastoid complex; **pf**, pterygoid fossa; **pgf**, postglenoid fossa; **oc**, occipital bone; **pt**, periotic part of the petromastoid complex; **ptb**, pterygoid bridge; **ptr**, pterygoid ridge; **sq**, squamosal; **srza**, squamosal root of zygomatic arch; **stf**, stapedial foramen; **th**, tympanic hook; **trc**, transverse canal.

Morphological Methods

External measurements (in millimeters) were taken in the field from fresh specimens, including total length (TOTAL), length of tail (TAIL), length of hind foot including claws (LHF), length of ear from notch (EAR), and weight in grams (WT); field catalogs of the collectors with these measurements and additional notes have been deposited at FMNH or USNM. Additional measurements of length of overfur (LOF, measured in the middorsal region) and number of tail scale rings per centimeter (TSR, counted at a point on the tail one-third of the total length from the base) were taken from fluid specimens preserved in 70% ethyl alcohol. The length of head and body (HBL) is the difference of the length of tail subtracted from total length.

Scanning electron micrographs of crania, mandibles, and teeth were made from uncoated specimens with an AMRAY 1810 scanning electron microscope.

Eighteen cranial and dental measurements of 44 adult specimens were taken with a digital caliper and recorded to the nearest 0.01 mm by Heaney, following the terminology and limits of these measurements defined in Heaney et al. (2011; see also Musser and Heaney, 1992): alveolar length of the maxillary molariform teeth (M1–M3), basioccipital length (BOL), breadth across upper incisors near their tips (BIT), breadth of first upper molar (BM1), breadth of zygomatic plate (BZP), height of braincase (HBC), interorbital breadth (IB), length of diastema (LD), length of incisive foramina (LIF), length of nasal bones (LN), lingual palatal breadth at the upper third molar (LBM3), mastoid breadth (MB), orbito-temporal length (OL), labial palatal breadth at M1 (PBM1), postpalatal length (PPL), rostral depth (RD), rostral length (RL), and zygomatic breadth (ZB). The number of measured adult specimens is less than the total number of specimens because we did not remove and clean skulls from immature individuals or adults with trap-damaged skulls.

Descriptive statistics (mean, standard deviation, and range) of cranial and dental measurements were calculated from sample groups. We assessed quantitative phenetic variation through principal components analysis (PCA), using the correlation matrix of $\log_{10}$-transformed measurements of adult specimens, using SYSTAT 10 for Windows (SPSS, Inc., 2000).

Karyology Methods

We prepared karyotypes from bone marrow cells following in vivo methodology (Patton, 1967, as modified by Rickart et al., 1989). Freshly killed animals captured in snap traps were processed using a modified in vitro technique (Rickart et al., 1998). Standard giemsa-stained karyotypes were prepared in the laboratory from fixed-cell suspensions. A minimum of 10 chromosome spreads was examined from each preparation. Chromosome terminology follows Rickart and Musser (1993). Because sex chromosomes could not be identified with certainty in many karyotypes, fundamental number (FN) refers to the total number of chromosome arms (including those of the sex chromosomes). Microscope slides and photomicrographs cross-referenced to voucher specimens at FMNH and USNM are housed at the Utah Museum of Natural History, University of Utah, Salt Lake City.

Molecular Genetic Methods

We used DNA sequences from the mitochondrial cytochrome *b* and the nuclear IRBP gene to infer phylogenetic relationships for members of the "vermivore clade" of Philippine endemic

rodents (Clade D of Jansa et al., 2006). Our cytochrome *b* data set comprised 58 specimens, including at least one representative of all recognized species of *Chrotomys*, *Rhynchomys*, and *Archboldomys,* as well as several new specimens whose phylogenetic position in this clade was uncertain. In addition, we included sequences from seven species of *Apomys*. We also used sequences from *Batomys* and *Phloeomys*—members of the cloud rat clade (Clade E)—as outgroups to root our phylogenetic analyses (Jansa et al., 2006; Rowe et al., 2008). Our IRBP data set comprised 19 specimens that were a subset of the larger cytochrome *b* data set. These 19 specimens were chosen as representative individuals from the set of newly collected specimens, and included sequences from exemplar species of *Rhynchomys* and *Apomys,* as well as from all recognized species of *Archboldomys* and *Chrotomys* (see Jansa and Weksler, 2004).

DNA was extracted using a Qiagen DNA Minikit (Qiagen, Inc.) from tissue preserved in 95% ethanol. We amplified and sequenced the complete cytochrome *b* gene using primers and PCR conditions, as described in Jansa et al. (2006).

DNA sequences were aligned using MUSCLE (Edgar, 2004) with default settings as implemented in Geneious v. 5.4.5 (Drummond et al., 2006). Where necessary, alignments were adjusted with reference to translated amino acid sequences for each gene. We analyzed each gene data set using maximum parsimony (MP) and maximum likelihood (ML) methods of phylogenetic inference. Analyses using MP were performed in PAUP* v4.0b10 (Swofford, 2002) using heuristic searches with 1000 replicates of random taxon addition and TBR branch swapping. For the ML analyses, we determined the best-fitting model of sequence substitution among the models available in MrModelTest ver. 2.3 (Nylander, 2004) using the Akaike Information Criterion (AIC). We specified this model in an ML search in GARLI ver. 2.0 (Zwickl, 2006). Nodal support values were estimated using 1000 bootstrap replicates for the MP analyses and 300 replicates for the ML analyses.

We also performed model-based (ML and Bayesian) phylogenetic analysis on the combined IRBP + cytochrome *b* gene data set. To do so, we evaluated the relative fit of four data-partitioning schemes: (1) a single partition including both genes; (2) two partitions, one for each gene; (3) three partitions, one for each codon position; and (4) six partitions, one for each codon position for each gene. We first determined the best-fitting model of sequence substitution for each possible partition separately, using the AIC in MrModelTest. To test the relative fit of the four broad partitioning schemes to our combined-gene data set, we calculated the log-likelihood of each using Bayesian inference in MrBayes 3.1.2 (Ronquist and Huelsenbeck, 2003). To do so, we specified the resulting best-fit sequence substitution model for each data partition as appropriate, and we unlinked all substitution parameters across partitions. We estimated branch lengths relative to each partition and allowed the substitution rate to vary among the specified partitions. For each partitioning scheme, we ran two chains of Metropolis-coupled Markov chain Monte Carlo (MC^3) for 3×10^6 generations, sampling every 100th generation. We discarded the first 10% of each run as burn-in and calculated the harmonic mean log-likelihood (HML) for each partitioning scheme using Tracer 1.4 (Rambaut and Drummond, 2007). The resulting HML values were used to calculate the AIC and Bayesian information criterion (BIC) scores for each partition (McGuire et al., 2007); the partitioning

scheme with the lowest AIC and BIC scores was then specified in a second Bayesian run with 10×10^6 generations of MC^3.

We also used this optimal partitioning scheme in a partitioned ML analysis as implemented in GARLI ver. 2.0 (Zwickl, 2006). We specified the best-fit model for each partition and allowed the model parameters to be estimated from the data. We performed five independent search replicates, but did not otherwise alter the default conditions for the tree search algorithm; nodal support values were obtained based on 100 bootstrap replicates.

RESULTS

Morphological Comparisons

Substantial variation exists among adults of six putative species of shrew mice from Luzon in external, cranial, and dental measurements (tables 1–4). Males tend to average only slightly larger than females, so we pooled the measurements of both sexes for multivariate analyses.

A principal components analysis, conducted on 18 cranial and dental measurements (log_{10}-transformed) of 44 adult specimens of shrew mice having intact (or nearly intact) crania included *Archboldomys luzonensis* from Carmarines Sur Province (*N* = 7), *A. maximus,* n. sp., from Mt. Amuyao, Mountain Province (*N* = 5),"*A.*" *musseri* from Cagayan Province (*N* = 2), "*A.*" *kalinga* from Mt. Bali-it, Kalinga Province (*N* = 12), *Soricomys montanus*, n. gen. and n. sp., from Mt. Pulag, Benguet Province, and Mt. Amuyao, Mountain Province (*N* = 10), and *Soricomys leonardocoi*, n. gen. and n. sp., from the Mingan Mountains, Aurora Province (*N* = 8). The first four components accounted for 87.6 % of the total variance (table 5). Most variables had positive loadings of high magnitude on the first component (accounting for 63.8% of the variance), indicating that much of the variation was related to size. The exceptions, with low loadings, were diastema length, postpalatal length, and breadth of incisors (which had a slight negative loading). The second component (accounting for 10.1% of the variation) had high-magnitude positive loadings for basioccipital length, diastema length, postpalatal length, and breadth of the upper incisors, separating individuals with large skulls, relatively elongate diastemas and postpalatal regions, and broad upper incisors from individuals having the converse. The third component (8.9% of the variance) had high-magnitude positive loadings for postpalatal length, mastoid breadth, and basioccipital length, but high-magnitude negative loadings for diastema length, length of incisive foramina, and incisor width, which distinguishes individuals with the combination of elongate skulls and postpalatal regions, broad mastoid regions, short diastemas, short incisive foramina, and narrow upper incisors from individuals having the converse. The fourth and following components had eigenvalues below 1.0, and so are not interpretable.

A bivariate plot of specimen scores on the first and second components (fig. 4) shows clear separation of the six putative taxa into four groupings. On the first component, expressing mainly size variation, specimens of *A. luzonensis* together with *A. maximus*, n. sp., from Mt. Amuyao are clearly distinct from a group consisting of "*A.*" *kalinga*, "*A.*" *musseri*, and specimens from the southern Central Cordillera (*Soricomys montanus*, n. sp.) and from the Mingan Mountains (*Soricomys leonardocoi*, n. sp.). The second component separates *A. luzonensis* from

A. maximus, and the Mingan series (*S. leonardocoi*, n. sp.) from a grouping that includes "*A.*" *kalinga*, "*A.*" *musseri*, and *S. montanus*, n. sp. *Archboldomys maximus*, n. sp., "*A.*" *kalinga*, "*A.*" *musseri, and S. montanus*, n. sp, have relatively elongate skulls, diastemas, and postpalatal regions, along with broad incisors compared with *A. luzonensis* and *S. leonardocoi*, n. sp., which have the opposite configuration for these variables.

In a plot of specimen scores on the first and third components (fig. 4B), component 3 separates *A. luzonensis* at one extreme from *A. maximus*, n. sp., and *S. leonardocoi*, n. sp., at the other, while "*A.*" *kalinga*, "*A.*" *musseri*, and *S. montanus*, n. sp., have intermediate scores that overlap with each other.

A principal components analysis (PCA) of the two species of *Archboldomys* sensu stricto as defined below (*A. luzonensis* and *A. maximus*; not shown) yielded results similar to those in the PCA of all six species. The two species are easily distinguished from each other on the first

TABLE 1. External measurements (mm), body mass (g), and measurement ratios (expressed as percentages) of adult *Archboldomys*, including *A. maximus*, n. sp.

Variables defined in Methods. First line of each variable gives the mean $\pm$ 1SD for sample size $N \geq 4$, or the average for $N \leq 3$; second line gives the range and sample size $< N$ (in parentheses).

Variable	*Archboldomys luzonensis* Mt. Isarog		*Archboldomys maximus*, n. sp. Mt. Amuyao		
	M ($N = 6$)[a]	F ($N = 2$)[b]	M (holotype)[c]	M ($N = 4$)[d]	F ($N = 4$)[e]
TOTAL	179.4 $\pm$ 9.24	177.0	213	213.0 $\pm$ 8.60	211.8 $\pm$ 14.10
	167–190 (5)	176–178		203–224	200–232
HBL	105.0 $\pm$ 4.06	106.5	114	115 $\pm$ 4.66	111.8 $\pm$ 9.11
	101–111 (5)	105–108		105–116	102–124
TAIL	74.4 $\pm$ 5.68	70.5	99	101.5 $\pm$ 8.54	100.0 $\pm$ 5.89
	66–80 (5)	70–71		90–108	94–108
TAIL/HBL (%)	65–75 (5)	65–68	87	80–103	85–96
LHF	28.0 $\pm$ 0.63	27.0	30	30.5 $\pm$ 1.73	30.5 $\pm$ 1.73
	27–29	27–27		29–33	29–33
LHF/HBL (%)	25–29 (5)	25–26	26	26–29	27–28
EAR	16.5 $\pm$ 0.55	17.0	20	19.5 $\pm$ 0.58	19.5 $\pm$ 1.29
	16–17	17–17		19–20	18–21
WEIGHT	34.3 $\pm$ 2.05	35.0	45.5	46.0 $\pm$ 2.16	44.5 $\pm$ 7.05
	31–36 (5)	33–37		43–48	40–55
LOF	08–11 (3)	—	10–11	10–13	09–11
TSR	15–16	—	20	20–24	18–22

[a]FMNH 95122 (holotype), 147172, 147173, USNM 573505, 573835, 573837.
[b]USNM 573838, 573840.
[c]FMNH193531.
[d]FMNH 193524, 193526, 193530, 193543.
[e]FMNH 193523, 193525, 193529, 193544.

TABLE 2. Cranial and dental measurements (mm) of adult *Archboldomys*, including *A. maximus*, n. sp.

Variables defined in Methods. First line of each variable gives the mean ± 1SD for sample size $N \geq 4$, or the average for $N \leq 3$; second line gives the range and sample size < N (in parentheses).

| | *Archboldomys luzonensis* | | *Archboldomys maximus*, n. sp. | | |
| | Mt. Isarog | | Mt. Amuyao | | |
Variable	M ($N = 6$)[a]	F ($N = 2$)[b]	M (holotype)[c]	M ($N = 2$)[d]	F ($N = 3$)[e]
BOL	25.68 ± 0.62	25.34	28.29	28.00	27.30
	24.78–26.25	25.04–25.63		27.88–28.12	26.98–27.63
IB	5.39 ± 0.14	5.55	5.67	5.70	5.66
	5.18–5.61	5.51–5.58		5.67–5.73	5.59–5.78
ZB	13.30 ± 0.20	13.41	14.17	14.20	13.85
	13.02–13.61	13.30–13.52		13.98–14.41	13.62–14.30
MB	11.75 ± 0.17	11.69	12.92	13.09	12.85
	11.60–12.06	11.69–11.69		12.98–13.20	12.48–13.24
LN	9.61 ± 0.29	9.72	10.30	10.98 (1)	10.29
	9.26–10.03 (5)	9.42–10.02			9.97–10.51
LIF	4.22 ± 0.08	4.31	4.20	3.98	3.82
	4.11–4.32	4.28–4.34		3.85–4.11	3.65–4.03
RD	5.27 ± 0.13	5.16	5.34	5.39	5.20
	5.10–5.47	5.10–5.22		5.30–5.47	5.13–5.33
RL	10.57 ± 0.37	10.56	11.95	12.24 (1)	11.67
	10.02–11.07 (5)	10.37–10.74			11.53–11.79
OL	9.00 ± 0.26	8.92	9.03	8.93	8.48
	8.67–9.28	8.83–9.00		8.88–8.97	8.21–8.69
M1–M3	4.62 ± 0.15	4.69	4.74	4.83	4.70
	4.43–4.80 (5)	4.67–4.70		4.72–4.93	4.63–4.85
PBM1	5.74 ± 0.10	5.83	6.02	5.76	5.84
	5.62–5.88	5.79–5.86		5.63–5.89	5.73–5.94
LD	6.82 ± 0.24	6.94	7.06	7.06	6.67
	6.55–7.15	6.81–7.07		6.99–7.13	6.24–6.99
PPL	9.48 ± 0.31	9.07	10.85	10.85	10.28
	9.06–9.90	8.83–9.31		10.79–10.91	10.03–10.44
LBM3	3.43 ± 0.24	3.56	3.58	3.40	3.39
	3.11–3.77	3.37–3.75		3.39–3.41	3.24–3.65
HBC	8.94 ± 0.16	8.82	9.24	9.04	9.12
	8.64–9.07	8.78–8.85		8.82–9.26	9.11–9.13
BM1	1.69 ± 0.04	1.71	1.84	1.78	1.74
	1.62–1.72	1.70–1.72		1.76–1.79	1.68–1.81
BIT	1.67 ± 0.06	1.62	1.67	1.70	1.67
	1.57–1.74	1.58–1.66		1.65–1.75	1.60–1.71
BZP	1.97 ± 0.07	2.00	1.91	1.76	1.83
	1.89–2.05	1.97–2.03		1.65–1.87	1.69–1.92

[a]FMNH 95122 (holotype), 147172, 147173; USNM 573505, 573835, 573837.
[b]USNM 573838, 573840.
[c]FMNH 193531.
[d]FMNH 193526, 193543.
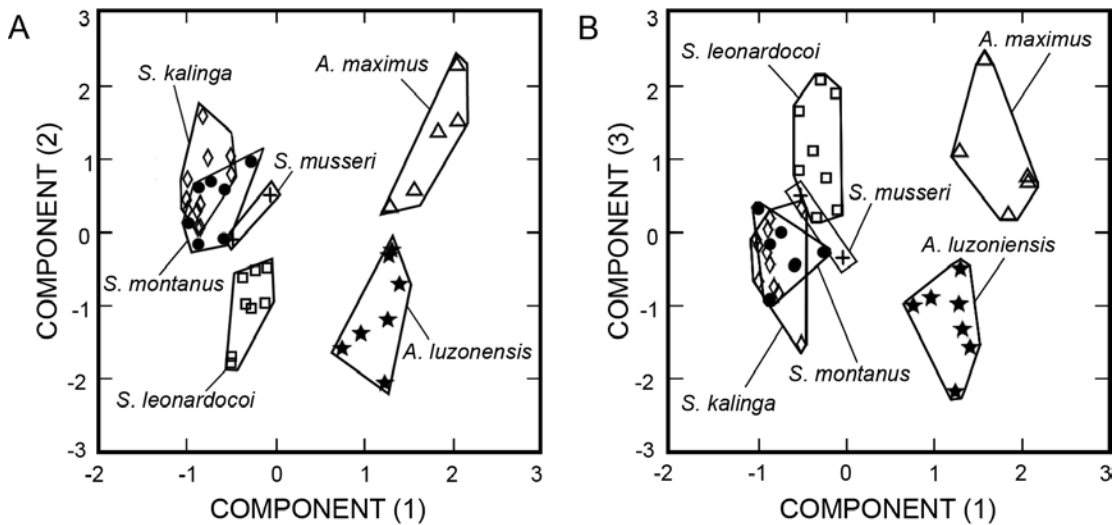[e]FMNH 193523, 193529, 193544.

FIG. 4. Projection of specimen scores onto the first two axes (**A**) and the first and third axes (**B**) of a principal components analysis of 18 cranial variables (log_{10}-transformed) from 44 specimens representing two putative species of *Archboldomy*s and four of *Soricomys*. Each species is shown enclosed in a maximally inclusive polygon.

component, which primarily reflects overall size, but with low loadings (which signifies overall size-independent variation) in rostral depth, orbito-temporal length, diastema length, lingual breadth of palate at M3, and breadth of incisors near their tips. Variation on the second, third, and fourth components showed extensive overlap; we suspect that this reflects age and individual variation.

A PCA of the four putative species referred below to *Soricomys,* n. gen. (table 6, fig. 5), using the same set of cranial and dental measurements, showed many of the same features as those evident in the PCA just described (table 5, fig. 4). The first four components accounted for 71.4% of the total variance (table 6). Most variables had moderate to high loadings on the first component, which accounted for 36.5% of the variance, indicating that most of the variance is size related, but diastema length had a strong negative loading, and breadth of incisors at their tips had a moderate negative loading, which indicates an inverse relationship with size for those two variables. Five variables (zygomatic breadth, nasal length, rostral depth, postpalatal length, and zygomatic plate breadth) had low loadings, which indicate that their variation occurs mostly independently of the component that reflects general size. The second component (15.1% of the variance) showed high loadings for basioccipital length, rostral depth, rostral length, diastema length, and breadth of incisors near the tip. The third component (10.1% of the variance) had strong negative loadings for zygomatic breadth, orbito-temporal length, lingual palatal breadth at M3, and breadth of incisors at their tips. The fourth component (9.7% of the variance) had strong negative loadings for postpalatal length and breadth of zygomatic plate, and a moderate negative loading for basioccipital length.

A plot of the scores of individual specimens on component 1 vs. component 2 (fig. 5A) shows clear separation of *S. leonardocoi,* n. sp., from the others, based on relatively high scores

TABLE 3. External measurements (mm), body mass (g), and measurement ratios (expressed as percentages) of adult *Soricomys*, n. gen., including *S. montanus*, n. sp., and *S. leonardocoi*, n. sp.

Variables defined in Methods. First line of each variable gives the mean ± 1SD for sample size $N \geq 4$, or the average for $N \leq 3$; second line gives the range and sample size $< N$ (in parentheses).

Variable	*Soricomys kalinga* Mt. Bali-it M (N=8)[a]	F (N=4)[b]	*Soricomys montanus*, n. sp. Mt. Data M (holotype)[c]	Mt. Amuyao M (N=2)[d]	F (N=2)[e]	Mt. Data M (N=5)[f]	Mt. Pulag M (N=1)[g]	*Soricomys musseri* Mt. Cetaceo M (N=2)[h]	*Soricomys leonardocoi*, n. sp. Mt. Mingan M (holotype)[i]	M (N=7)[j]	F (N=6)[k]
TOTAL	197.9 ± 4.98 191–207 (7)	188.7 183–193 (3)	188	191.0 190–192	182.5 182–183	190.6 ± 4.78 188–199	174	189.0 180–198	195	201.0 ± 4.55 198–208	188.2 ± 5.91 180–195
HBL	102.3 ± 5.34 93–108 (7)	99.0 98–100 (3)	93	95.5 95–96	95 95 (1)	99.6 ± 4.22 93–103	87	98.0 91–105	103	108.1 ± 5.08 103–115	103.8 ± 3.54 98–107
TAIL	95.6 ± 3.64 90–101 (7)	89.8 ± 3.69 85–94	95	95.5 95–96	88 87–89	91.0 ± 5.87 85–98	87	91.0 89–93	92	92.9 ± 3.24 86–95	84.3 ± 2.94 82–88
TAIL/HBL (%)	84–105	87–95	102	100	92 (1)	82–102	100	89–98	89	75–92	77–84
LHF	23.8 ± 1.16 22–26	22.5 ± 0.58 22–23	23	24.5 24–25	23.5 23–24	23.6 ± 1.14 22–25	23	20.0 19–21	25	24.0 ± 1.41 21–25	23.3 ± 0.82 22–24
LHF/HBL (%)	21–26	22–23 (3)	25	25–26	24 (1)	22–25	26	18–23	24	19–24	21–24
EAR	13.9 ± 0.64 13–15	14.0 ± 0.82 13–15	14	14.5 14–15	13.5 13–14	14.4 ± 0.55 14–15	13	14.0 14–14	14	14.3 ± 0.49 14–15	13.8 ± 0.41 13–14
WEIGHT	27.4 ± 1.24 26–29	22.8 ± 1.50 21–24	27	25.5 25–26	27 25–29	28.0 ± 3.16 23–31	20	32 (1)	33	32.9 ± 1.95 31–36	30.3 ± 2.73 26–34

| Variable | *Soricomys kalinga* Mt. Bali-it | | *Soricomys montanus*, n. sp. | | | | | *Soricomys musseri* Mt. Cetaceo | *Soricomys leonardocoi*, n. sp. Mt. Mingan | | |
| | | | Mt. Data | Mt. Amuyao | | Mt. Data | Mt. Pulag | | | | |
	M (N = 8)[a]	F (N = 4)[b]	M (holotype)[c]	M (N = 2)[d]	F (N = 2)[e]	M (N = 5)[f]	M (N = 1)[g]	M (N = 2)[h]	M (holotype)[i]	M (N = 7)[j]	F (N = 6)[k]
LOF	07–08 (4)	07–09 (3)	08 – 09	08–09	07–08	08–09	09–10	08–09	09–10	09–11	08–10
TSR	21–24 (4)	22 (3)	24	21	24	22–27	23	24–26	22	22–24	24–25

[a] FMNH 167304, 167308, 169124, 170967, 175554, 175555 (holotype), 175720, 175721.
[b] FMNH 167307, 170966, 175552, 175558.
[c] FMNH 188314.
[d] FMNH 193514, 193520.
[e] FMNH 193515, 193521.
[f] FMNH 188313–188315, 188319, 188449.
[g] FMNH 198715.
[h] FMNH 147176 (holotype), 185909.
[i] FMNH 190972.
[j] FMNH 190962, 190963, 190968, 190972 (holotype), 190973, 190977, 190982.
[k] FMNH 190961, 190964, 190965, 190970, 190979, 190981.

TABLE 4. Cranial and dental measurements of adult *Soricomys*, n. gen., including *S. montanus*, n. sp., and *S. leonardocoi*, n. sp.

Variables defined in Methods. First line of each variable gives the mean ± 1SD for sample size $N \geq 4$, or the average for $N \leq 4$; second line gives the range and sample size < N (in parentheses).

| | Soricomys kalinga | | | Soricomys montanus, n. sp. | | | | Soricomys musseri | Soricomys leonardocoi, n. sp. | | |
| | Mt. Bali-it | | Mt. Data | Mt. Amuyao | | Mt. Data | Mt. Pulag | Mt. Cetaceo | | Mt. Mingan | |
Variable	M (N =8)[a]	F (N =4)[b]	M (holotype)[c]	M (N =2)[d]	F (N =1)[e]	M (N =5)[f]	M (N =1)[g]	M (N =2)[h]	M (holotype)[i]	M (N =3)[j]	F (N =4)[k]
BOL	25.24 ± 0.43 24.69–25.78	24.88 ± 0.18 24.68–25.04	25.74	25.22 25.02–25.41	24.59	25.43 ± 0.37 25.02–25.78	24.88	25.52 25.43–25.60	24.97	25.54 25.42–25.65	25.23 ± 0.42 24.72–25.71
IB	4.74 ± 0.09 4.64–4.91	4.62 ± 0.11 4.48–4.74	4.78	4.81 4.79–4.82	4.77	4.99 ± 0.12 4.78–5.10	4.86	5.02 4.88–5.15	4.95	5.11 5.05–5.20	5.13 ± 0.08 5.05–5.23
ZB	11.91 ± 0.32 11.49–12.49	11.83 ± 0.20 11.52–11.95	11.50	11.82 11.64–11.99	11.73	11.81 ± 0.30 11.47–12.06	11.29	12.09 11.64–12.53	11.72	11.62 10.99–11.98	11.84 ± 0.09 11.72–11.94
MB	10.83 ± 0.19 10.61–11.15	10.65 ± 0.13 10.48–10.80	11.00	10.91 10.76–11.06	10.69	11.04 ± 0.20 10.81–11.32	10.46	11.16 11.00–11.31	11.14	11.13 11.06–11.19	11.24 ± 0.08 11.13–11.29
LN	8.95 ± 0.19 8.75–9.30 (7)	8.87 ± 0.13 8.72–9.02	9.20	8.81 8.72–8.89	8.52	9.02 ± 0.22 8.78–9.21 (4)	9.32	9.43 9.07–9.78	9.04	8.84 8.68–8.95	8.98 ± 0.30 8.56–9.27
LIF	3.19 ± 0.17 3.00–3.56	3.15 ± 0.04 3.11–3.21	3.52	3.06 3.01–3.11	3.32	3.33 ± 0.21 3.09–3.52	3.10	3.23 3.19–3.26	3.45	3.43 3.36–3.52	3.38 ± 0.10 3.28–3.52
RD	4.71 ± 0.12 4.58–4.90	4.58 ± 0.15 4.41–4.72	4.87	4.61 4.57–4.65	4.58	4.87 ± 0.11 4.74–5.04	4.64	4.56 4.50–4.62	4.29	4.57 4.50–4.64	4.51 ± 0.07 4.46–4.61
RL	9.15 ± 0.20 8.87–9.42 (7)	8.91 ± 0.14 8.71–9.05	9.44	9.06 8.97–9.15	8.71	9.33 ± 0.32 9.05–9.73 (4)	9.32	9.25 8.97–9.52	9.22	9.27 9.07–9.42	9.09 ± 0.24 8.81–9.38
OL	8.57 ± 0.27 8.23–9.12	8.46 ± 0.31 8.08–8.76	8.23	8.22 8.21–8.22	8.14	8.32 ± 0.14 8.21–8.53	8.40	8.87 8.79–8.95	8.73	8.75 8.60–8.85	8.63 ± 0.09 8.55–8.75
M1–M3	3.82 ± 0.08 3.72–3.93	3.80 ± 0.08 3.74–3.90	3.90	3.82 3.77–3.87	3.89	3.86 ± 0.10 3.73–4.00	3.73	4.01 3.97–4.05	4.16	4.18 4.10–4.30	4.17 ± 0.06 4.09–4.22
PBM1	4.52 ± 0.14 4.31–4.76	4.55 ± 0.08 4.47–4.64	4.56	4.51 4.46–4.55	4.53	4.66 ± 0.12 4.51–4.79	4.58	4.93 4.78–5.07	4.87	4.99 4.90–5.07	5.01 ± 0.12 4.86–5.15
DL	6.86 ± 0.31 6.58–7.42	6.74 ± 0.10 6.64–6.87	7.05	6.69 6.67–6.71	6.77	6.99 ± 0.12 6.82–7.10	6.80	6.70 6.66–6.70	6.26	6.48 6.37–6.59	6.46 ± 0.14 6.31–6.63
PPL	9.94 ± 0.13 9.70–10.10	9.86 ± 0.11 9.76–10.01	9.62	9.79 9.67–9.91	9.47	9.68 ± 0.15 9.50–9.88	9.59	9.91 9.80–10.01	9.78	10.15 9.96–10.30	9.78 ± 0.30 9.52–10.14
LBM3	3.18 ± 0.05 3.12–3.27	3.23 ± 0.13 3.04–3.32	3.17	3.17 2.99–3.35	3.22	3.24 ± 0.05 3.17–3.30	3.28	3.34 3.28–3.40	3.23	3.26 3.19–3.40	3.29 ± 0.04 3.26–3.34
HBC	7.64 ± 0.26 7.21–7.95	7.39 ± 0.24 7.16–7.63	7.70	7.75 7.70–7.80	7.89	7.77 ± 0.11 7.70–7.95	7.47	8.21 8.18–8.24	7.79	8.06 7.83–8.27	8.05 ± 0.08 7.94–8.14
BM1	1.16 ± 0.04 1.10–1.20	1.15 ± 0.02 1.13–1.17	1.20	1.19 1.17–1.20	1.15	1.22 ± 0.03 1.18–1.26	1.17	1.24 1.22–1.25	1.30	1.31 1.30–1.32	1.32 ± 0.04 1.28–1.37
BIT	1.76 ± 0.10 1.66–1.99	1.76 ± 0.06 1.68–1.81	1.66	1.73 1.69–1.77	—	1.72 ± 0.04 1.66–1.77	1.62	1.76 1.67–1.84	1.48	1.58 1.47–1.69	1.59 ± 0.09 1.47–1.69

| Variable | Soricomys kalinga Mt. Bali-it | | Soricomys montanus, n. sp. | | | | | Soricomys musseri Mt. Cetaceo | Soricomys leonardocoi, n. sp. | | |
| | | | Mt. Data | Mt. Amuyao | | Mt. Data | Mt. Pulag | | | Mt. Mingan | |
	M (N=8)[a]	F (N=4)[b]	M (holotype)[c]	M (N=2)[d]	F (N=1)[e]	M (N=5)[f]	M (N=1)[g]	M (N=2)[h]	M (holotype)[i]	M (N=3)[j]	F (N=4)[k]
BZP	1.54 ± 0.09 1.42–1.66	1.56 ± 0.04 1.52–1.62	1.49	1.53 1.51–1.53	1.37	1.45 ± 0.09 1.35–1.56	1.50	1.47 1.44–1.49	1.47	1.63 1.58–1.68	1.57 ± 0.09 1.46–1.69

[a]FMNH 167304, 167308, 169124, 170967, 175554, 175555 (holotype), 175720, 175721.
[b]FMNH 167307, 170966, 175552, 175558.
[c]FMNH 188314.
[d]FMNH 193514, 193520.
[e]FMNH 193521.
[f]FMNH 188313–188315, 188319, 188449.
[g]FMNH 198715.
[h]FMNH 147176 (holotype), 185909.
[i]FMNH 190972.
[j]FMNH 190963, 190973, 190982.
[k]FMNH 190964, 190965, 190970, 190979.

TABLE 5. Results of principal components analyses of $\log_{10}$–transformed cranial and dental measurements of *Archboldomys* and *Soricomys* adults.

Shown are the character loadings, eigenvalues, and percentage of variance explained on the first three components.

Variable	Principal component		
	1	2	3
BOL	0.776	0.521	0.264
IB	0.917	-0.146	0.162
ZB	0.936	0.124	-0.089
MB	0.927	0.154	0.259
NL	0.878	0.247	0.092
LIF	0.891	-0.233	-0.233
RD	0.847	0.140	-0.302
RL	0.960	0.196	0.038
OL	0.510	-0.239	-0.203
M1–M3	0.944	-0.217	0.088
PBM1	0.968	-0.187	0.040
DL	0.172	0.528	-0.671
PPL	0.161	0.656	0.636
LBM3	0.605	-0.128	-0.267
HBC	0.949	-0.118	0.067
BM1	0.974	-0.163	0.030
BIT	-0.107	0.623	-0.509
ZP	0.850	-0.141	-0.181
Eigenvalue	11.477	1.819	1.599
Variance explained	63.8%	10.1%	8.9%

on the first component and low scores on the second component. *Soricomys musseri* is likewise distinct, scoring moderate to high on the first and second components. Specimens of *Soricomys kalinga* and *S. montanus,* n. gen. and n. sp., overlap broadly with each other, but are distinct from the other two putative species.

A plot of individuals on component 3 vs. component 4 (fig. 5B) shows separation of *S. kalinga* and *S. montanus,* n. gen. and n. sp., along component 3 for most individuals, though some overlap remains; this reflects the tendency of *S. kalinga* to have greater zygomatic breadth, orbito-temporal length, lingual palatal breadth at M3, and breadth of incisors near their tips than *S. montanus,* n. sp. The other species largely overlap on these components.

Karyology

Archboldomys luzonensis: As reported previously (Rickart and Musser 1993; Rickart and Heaney, 2002), the karyotype has 2N = 26 and FN = 43 (table 7). The autosomal complement

TABLE 6. Results of principle components analyses of $\log_{10}$–transformed cranial and dental measurements of *Soricomys* adults.

Shown are the character loadings, eigenvalues, and percentage of variance explained on the first four components.

Variable	Principle component			
	1	2	3	4
BOL	0.467	0.635	0.113	-0.497
IB	0.833	0.088	0.143	0.340
ZB	0.202	0.455	-0.650	0.173
MB	0.867	0.237	-0.035	0.039
NL	0.207	0.457	0.101	0.128
LIF	0.539	0.009	0.405	0.062
RD	-0.282	0.688	0.300	0.111
RL	0.413	0.751	0.269	-0.134
OL	0.487	-0.096	-0.586	-0.017
M1–M3	0.875	-0.263	0.026	-0.162
PBM1	0.947	-0.020	-0.068	0.006
DL	-0.611	0.567	0.238	-0.078
PPL	0.240	0.005	-0.065	-0.750
LBM3	0.471	0.247	-0.497	0.171
HBC	0.802	0.104	0.011	0.102
BM1	0.902	-0.174	0.193	0.128
BIT	-0.486	0.500	-0.569	-0.095
ZP	0.175	-0.231	-0.069	-0.798
Eigenvalue	6.561	2.726	1.816	1.741
Variance explained	36.5%	15.1%	10.1%	9.7%

includes eight pairs of small to large metacentric or submetacentric chromosomes and four pairs of very small to medium-sized telocentric chromosomes. A large submetacentric X chromosome is present in both sexes. It is paired with a medium-sized telocentric Y chromosome in males, and with a large telocentric element in the single female available (fig. 6A).

Soricomys kalinga, n. gen.: The karyotype of this species was reported previously (as *Archboldomys musseri*) by Rickart and Heaney (2002), based on a poor quality in vitro preparation. The karyotype has 2N = 44, consisting of small to large telocentric or subtelocentric chromosomes and some small submetacentric chromosomes. The X chromosome is tentatively identified as the largest element, and is either telocentric or subtelocentric. The Y chromosome is tentatively identified as small and telocentric. The FN has not been determined (fig. 6B).

Soricomys montanus, n. gen. and n. sp.: The karyotype has 2N = 44; FN = 52, with four pairs of submetacentric autosomes (two large and two small), 17 pairs of small to large telocentric or subtelocentric autosomes, a large telocentric or subtelocentric X chromosome, and a very small, apparently telocentric, Y chromosome (fig. 6C).
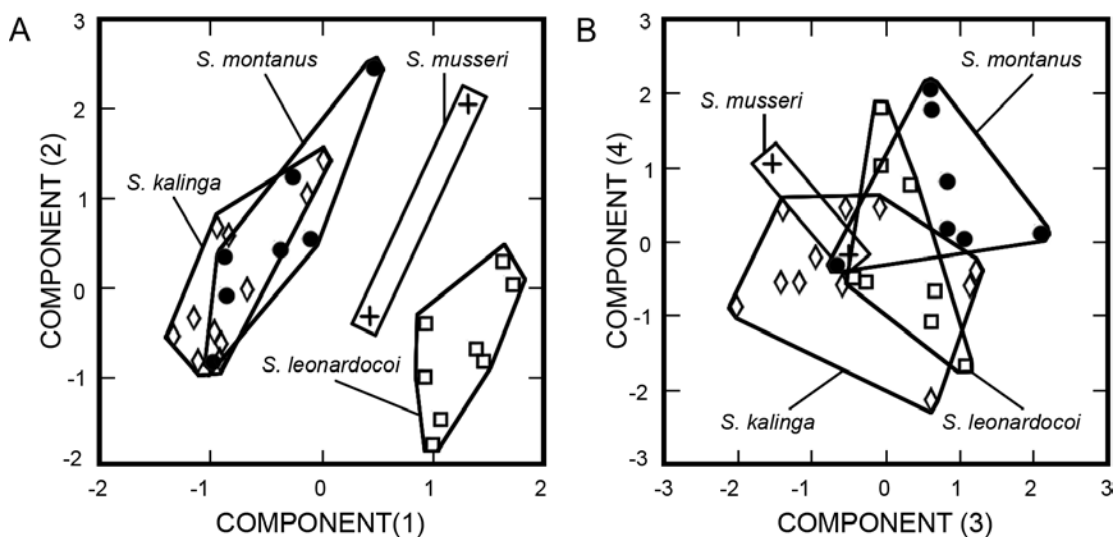
FIG. 5. Projection of specimen scores onto the first two axes (**A**) and the third and fourth axes (**B**) of a principal components analysis of 18 cranial variables ($\log_{10}$-transformed) from 32 specimens representing four putative species of *Soricomys,* n. gen. Each species is shown enclosed in a maximally inclusive polygon.

Molecular Phylogenetic Analysis

The cytochrome *b* data set yielded 394 parsimony-informative characters for the 56 ingroup and two outgroup taxa (table 8). Parsimony analysis of this data set resulted in seven minimum-length trees with length of 1610 steps, CI = 0.386, and RI = 0.817. The strict consensus of these seven trees differs topologically from the tree recovered from a maximum-likelihood analysis of the same data, but conflict is limited to poorly supported (bootstrap < 75%) nodes. We therefore present the maximum-likelihood tree annotated with support values from the parsimony analysis (fig. 7).

Among the available substitution models, a GTR + I + Γ_4 model of sequence evolution provided the best fit to the cytochrome *b* data (-lnL = 8261.366). Parameter estimates indicate that cytochrome *b* is markedly guanosine poor in these taxa and that transitions greatly outnumber transversions (table 9), which is consistent with estimates from other mammalian taxa. The tree derived from ML analysis of the cytochrome *b* data set (fig. 7) strongly supports monophyly of the genera *Rhynchomys*, *Chrotomys*, and *Apomys* (though a more rigorous test of *Apomys* monophyly is provided by Heaney et al., 2011). However, the four specimens from the type locality of *Archboldomys musseri* (DNA numbers DSB 3711, DSB 3747, DSB 3704, and PAA 609) do not cluster with other members of *Archboldomys* (including the type species, *A. luzonensis*). Rather, a clade comprising these four specimens—which are clearly assignable to a single species—join a well-supported clade (ML-bootstrap = 99%; MP-bootstrap = 100%) along with several newly collected specimens of small shrew mice, including specimens previously assigned as *A. kalinga* and *A. musseri*. We recognize this clade as a new genus comprising four species, as described below. In contrast, four specimens representing a large shrew mouse from Mt. Amuyao, Mountain

Province, cluster with each other and form a sister-taxon relationship with *A. luzonensis*. Uncorrected, pairwise cytochrome *b* distance between these two clades averages 9.2%, and the two taxa are morphologically easily distinguishable; we therefore recognize a new species of *Archboldomys*, as described below. Relationships among the five genera are generally not well supported by the cytochrome *b* data set. However, a sister-taxon relationship between *Chrotomys* and the new genus is recovered in both parsimony and ML analyses with moderate (MP-bootstrap = 72%) to strong (ML-bootstrap = 92%) support, but no other intergeneric relationship is recovered from these mitochondrial data with confidence (fig. 7).

The IRBP data set contained 81 parsimony-informative char-

FIG. 6. Karyotypes of *Archboldomys* and *Soricomys*. **A,** *A. luzonensis* male (USNM 573835) from Mt. Isarog: 2N = 26, FN = 43. **B,** *S. kalinga* male (FMNH 169122) from Mt. Bali-it: 2N = 44, FN unknown. **C,** *S. montanus* male (EAR 6308) from Mt. Amuyao: 2N = 44, FN = 52.

acters for the 19 included taxa. Parsimony analysis of this data set resulted in 30 minimum-length trees of 188 steps with CI = 0.883 and RI = 0.897; the strict consensus of these trees does not conflict with those derived from ML analysis at any well-supported node and is not discussed further. A two-rate HKY model with Γ_4 distributed rate variation provided the best fit to the IRBP data set (table 9). The tree resulting from ML analysis under this model (lnL = -2862.011; fig. 8A) is largely consistent with the tree based on cytochrome *b*. The IRBP data confirm that
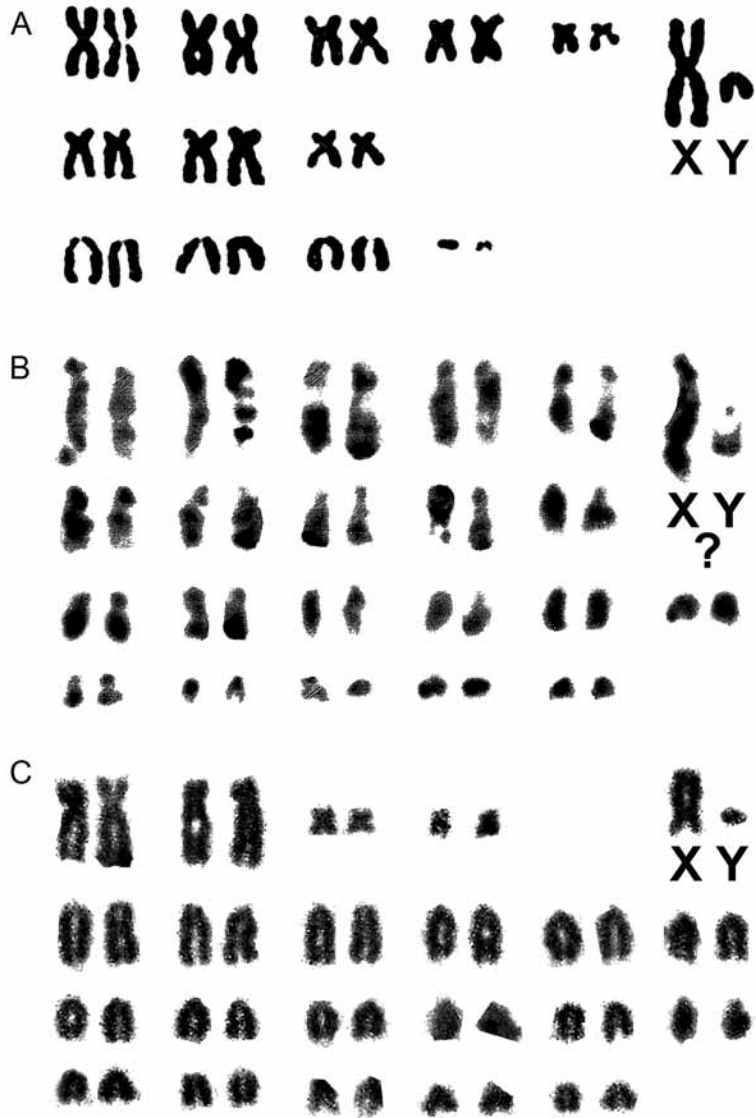
TABLE 7. Summary of karyotypic variation among members of the *Chrotomys* Division and *Crunomys suncoides*.

| Taxon	Island	Province	2N	M	SM	ST	T	X	Y	FN	Source
Apomys (Apomys) hylocoetes	Mindanao	Bukidnon	48	0	1	3	19	T	T	56	Rickart and Heaney, 2002
Apomys (Apomys) insignis	Mindanao	Bukidnon	36	5	3	9	0	ST	ST	72	Rickart and Heaney, 2002
Apomys (Apomys) musculus	Luzon	Camarines Sur	42	3	1	1	15	T	T	52	Rickart and Musser, 1993
Apomys (Apomys) sp.	Leyte	Leyte	44	3	1	17	0	ST	ST	88	Rickart and Musser, 1993
Apomys (Apomys) sp.	Negros	Negros Oriental	30	6	3	0	5	ST	SM	50	Rickart and Musser, 1993
Apomys (Megapomys) abrae	Luzon	Kalinga	44	1	2	2	16	T	T	54	Heaney et al., 2011
Apomys (Megapomys) banahao	Luzon	Quezon	48	2	0	0	21	SM	T	54	Heaney et al., 2011
Apomys (Megapomys) datae	Luzon	Mountain Prov.	44	1	1	3	16	T	T	54	Heaney et al., 2011
Apomys (Megapomys) zambalensis	Luzon	Bataan	44	2	1	3	15	SM	T	58	Heaney et al., 2011
Archboldomys luzonensis	Luzon	Camarines Sur	26	5	3	0	4	SM	T	43	Rickart and Musser, 1993
Chrotomys gonzalesi	Luzon	Camarines Sur	44	2	1	1	17	T	T	52	Rickart and Musser, 1993
Chrotomys mindorensis	Luzon	Bataan	44	2	1	1	17	T	T	52	Rickart (unpublished)
Chrotomys silaceus	Luzon	Kalinga	44	2	1	1	17	T	T	52	Rickart and Heaney, 2002
Chrotomys whiteheadi	Luzon	Kalinga	38	2	4	1	11	T	T	52	Rickart and Heaney, 2002
Crunomys suncoides	Mindanao	Bukidnon	36	0	0	0	17	T	T	36	Rickart and Heaney, 2002
Rhynchomys isarogensis	Luzon	Camarines Sur	44	2	1	1	17	T	T	52	Rickart and Heaney, 2002
Rhynchomys soricoides	Luzon	Mountain Prov.	44	2	1	?	?	T	T	54?	Rickart (unpublished)
Soricomys kalinga	Luzon	Kalinga	44							?	Rickart and Heaney, 2002
Soricomys montanus	Luzon	Mountain Prov.	44	2	1	1	17	T	T	52	this study
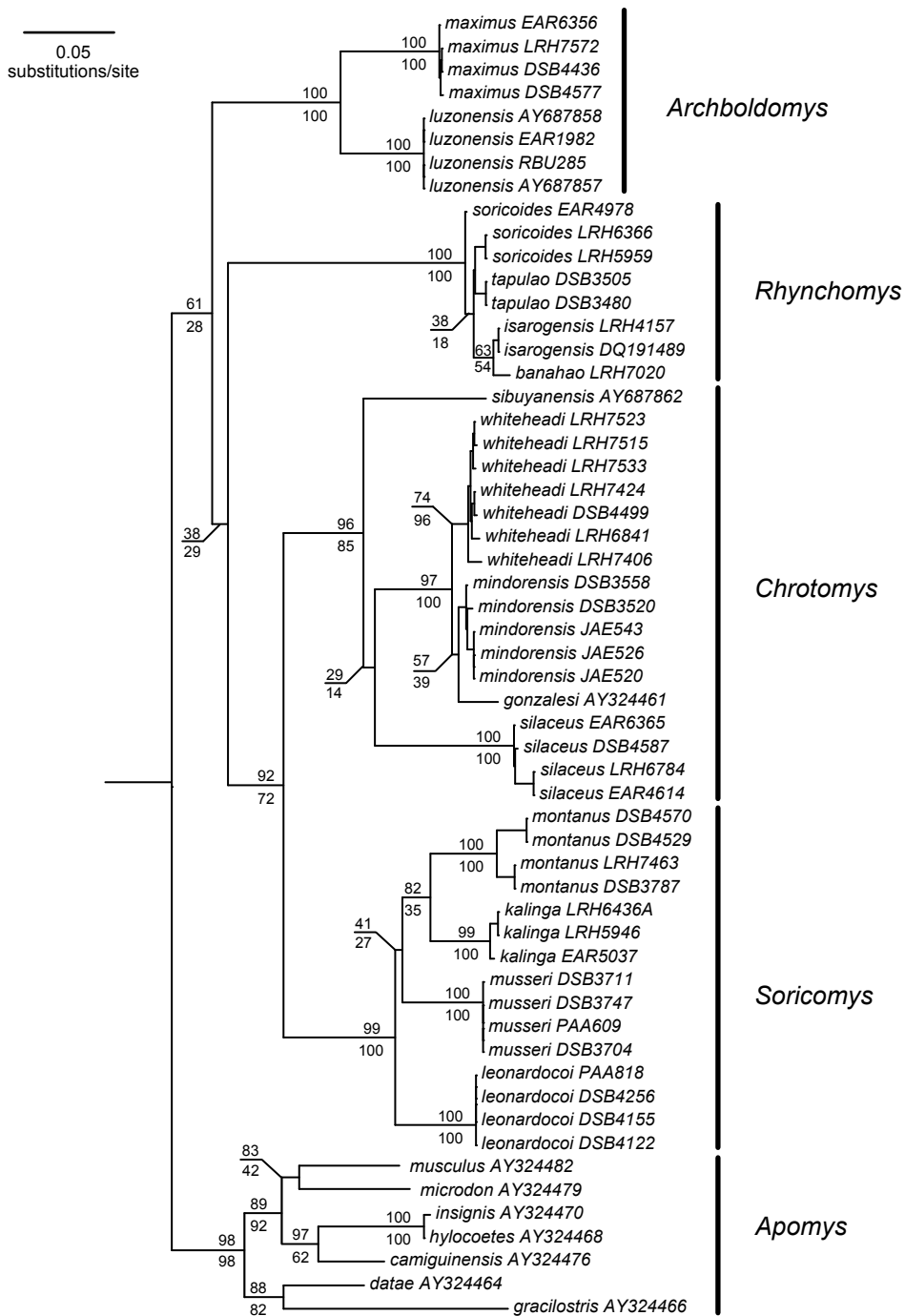
FIG. 7. The tree resulting from a maximum-likelihood analysis of the cytochrome *b* from *Chrotomys* Division species under the best-fitting model (GTR + I + Γ_4). Numbers at nodes indicate maximum-likelihood (above the line) or parsimony (below the line) bootstrap support. Terminal taxa are identified by species name and a unique alphanumeric identifier (either DNA number or Genbank accession number; table 6). Trees are rooted with *Phloeomys cumingi* and *Batomys granti* as outgroups (not shown).
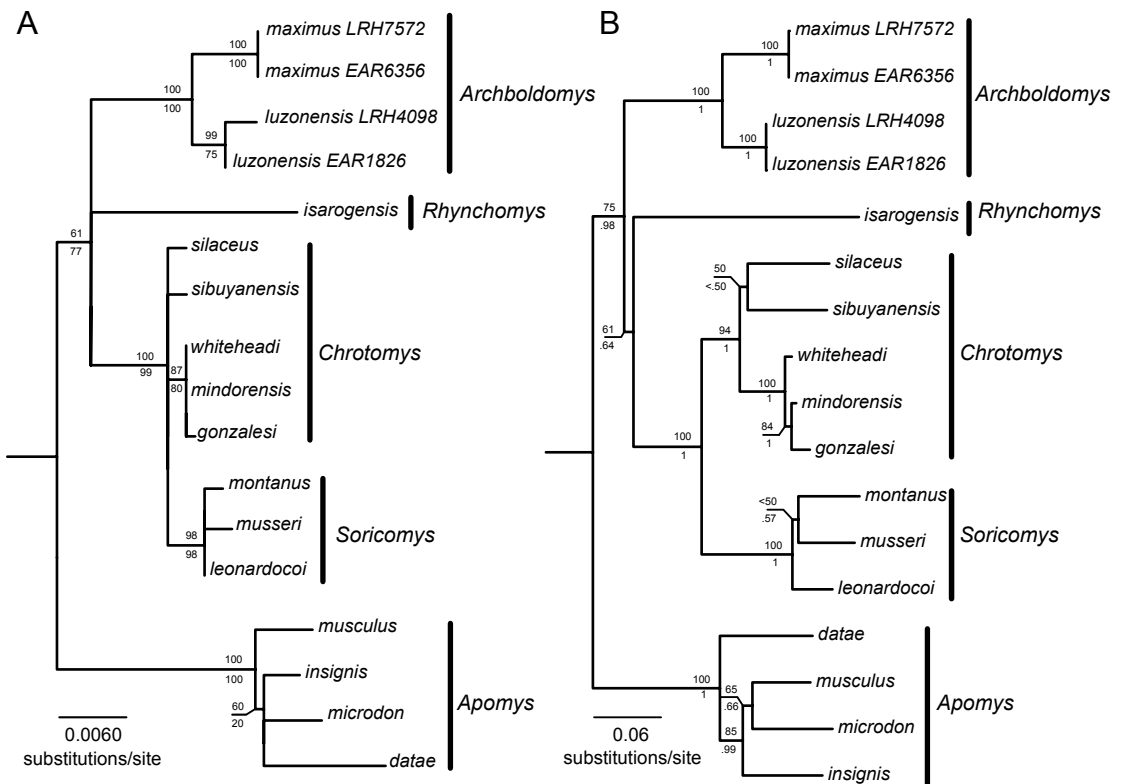
FIG. 8. **A,** The tree resulting from a maximum-likelihood analysis of the IRBP data set under the best-fitting model (HKY + Γ_4). Numbers at nodes indicate maximum-likelihood (above the line) or parsimony (below the line) bootstrap support. **B,** The tree resulting from a mixed-model maximum-likelihood analysis of the combined IRBP + cytochrome *b* data set. Numbers at nodes indicate maximum-likelihood bootstrap support (above the line) or posterior probabilities resulting from a mixed-model Bayesian analysis (below the line). Trees are rooted with *Phloeomys cumingi* and *Batomys granti* as outgroups (not shown).

specimens assigned to *A. kalinga* (assigned below to *Soricomys montanus*, n. sp.) and *A. musseri* are not closely related to the type species *A. luzonensis*, but are part of a distinct clade. In addition, these data also recover the sister-taxon relationship between *A. luzonensis* and the large shrew mouse from Mt. Amuyao. The IRBP data do not recover a monophyletic *Chrotomys*, but monophyly is not inconsistent with these data: *C. silaceus* and *C. sibuyanensis* form an unresolved polytomy with a clade comprising the remaining three species of *Chrotomys*. There is strong support for a sister-taxon relationship between the new genus and species of *Chrotomys*; otherwise, IRBP provides little additional support for intergeneric relationships.

A model that partitions the data set six ways (by gene and by codon) provided the best fit to the combined-gene data set (table 10). We implemented this partitioning scheme with the best-fit substitution model for each codon position (GTR + Γ_4: cytb-1; HKY + I: cytb-2, IRBP-3; GTR + I + Γ_4: cytb-3; GTR + I: IRBP-1, IRBP-2) in both maximum-likelihood and Bayesian mixed-model analysis; the maximum-likelihood tree (lnL = -8951.23) is shown in figure 8B with nodal Bayesian posterior probabilities indicated. Not surprisingly, this tree is highly congruent with

FIG. 9. View of the posterior edge of the upper incisors of **A,** *Archboldomys luzonensis* (FMNH 147172); **B,** *A. maximus,* n. sp. (FMNH 193531, holotype); **C,** *Soricomys kalinga* (FMNH 175555, holotype); **D,** *Soricomys leonardocoi,* n. sp. (FMNH 190972, holotype); **E,** *Soricomys montanus,* n. sp. (FMNH 188314, holotype); **F,** *Soricomys musseri* (FMNH 147176, holotype).

trees based on the individual gene data sets, and recovers the principle relationships discussed above. In addition, this tree provides additional intergeneric resolution: the split between *Apomys* and a clade comprising the remaining four genera receives some statistical support in this analysis (ML-bootstrap = 75%; BPP=0.98); however, relationships among *Archboldomys*, *Rhynchomys*, and the clade comprising *Chrotomys* and the new genus remain uncertain.

Taxonomy

Analyses of the combined morphological, chromosomal, and molecular data analyses of all representatives of the shrew mice of the Philippines strongly support the following taxonomic decisions: (1) redefinition of *Archboldomys*, (2) establishment of *Soricomys*, n. gen., described below, and (3) recognition of one new species of *Archboldomys* and two new species of *Soricomys,* n. gen. We emend the diagnoses of all previously recognized species of *Archboldomys* (*A. luzonensis*, "*A.*" *kalinga*, and "*A.*" *musseri*), and transfer two into the new genus *Soricomys* (*S. kalinga* and *S. musseri*).

Archboldomys Musser, 1982

Type Species: *Archboldomys luzonensis* Musser, 1982a: 30.

Included Species: Only the type species and *A. maximus,* n. sp.

Distribution: Known only from two mountains on Luzon Island: Mt. Isarog in southeastern Luzon and Mt. Amuyao in the Central Cordillera of northern Luzon (fig. 1).

TABLE 8. List of sequenced specimens.

Taxon	DNA No.[1]	Museum No.	cytochrome *b* source[2]	IRBP source[2]
Archboldomys maximus	EAR 6356	FMNH 193526	this study	this study
Archboldomys maximus	LRH 7572	FMNH 193522	this study	this study
Archboldomys maximus	DSB 4436	FMNH 193528	this study	
Archboldomys maximus	DSB 4577	FMNH 193944	this study	
Archboldomys luzonensis	LRH 4098	USNM 573834	AY687858[3]	DQ191495[4]
Archboldomys luzonensis	EAR 1982	USNM 573839	this study	
Archboldomys luzonensis	RBU 285	USNM 573836	this study	
Archboldomys luzonensis	EAR 1826	USNM 573835	AY687857[3]	EU349837[5]
Rhynchomys soricoides	EAR 4978	FMNH 175618	this study	
Rhynchomys soricoides	LRH 6366	FMNH 169170	this study	
Rhynchomys soricoides	LRH 5959	FMNH 167320	this study	
Rhynchomys tapulao	DSB 3505	FMNH 183555	this study	
Rhynchomys tapulao	DSB 3480	FMNH 183554	this study	
Rhynchomys isarogensis	LRH 4157	USNM 573577	this study	
Rhynchomys isarogensis	EAR 1833	USNM 573900	DQ191489[4]	AY326108[4]
Rhynchomys banahao	LRH 7020	FMNH 178429	this study	
Chrotomys gonzalesi	EAR 1850	USNM 458953		DQ191503[4]
Chrotomys gonzalesi	LRH 4176	USNM 458952	AY324461[6]	
Chrotomys sibuyanensis	SMG 5150	FMNH 145701	AY687862[3]	DQ191504[4]
Chrotomys whiteheadi	LRH 7523	FMNH 193960	this study	
Chrotomys whiteheadi	LRH 7515	FMNH 193737	this study	
Chrotomys whiteheadi	LRH 7533	FMNH 193962	this study	this study
Chrotomys whiteheadi	LRH 7424	FMNH 188360	this study	
Chrotomys whiteheadi	DSB 4499	FMNH 193748	this study	
Chrotomys whiteheadi	LRH 6841	FMNH 175575	this study	
Chrotomys whiteheadi	LRH 7406	FMNH 188458	this study	
Chrotomys mindorensis	DSB 3558	FMNH 183551	this study	
Chrotomys mindorensis	DSB 3520	FMNH 183549	this study	
Chrotomys mindorensis	JAE 543	KU 164432	this study	this study
Chrotomys mindorensis	JAE 526	KU 164431	this study	
Chrotomys mindorensis	JAE 520	KU 164430	this study	
Chrotomys silaceus	EAR 6365	FMNH 193714	this study	
Chrotomys silaceus	DSB 4587	FMNH 193734	this study	
Chrotomys silaceus	LRH 6784	FMNH 175723	this study	this study
Chrotomys silaceus	EAR 4614	FMNH 169132	this study	
Soricomys montanus	DSB 4570	FMNH 193521	this study	this study

Taxon	DNA No.[1]	Museum No.	cytochrome *b* source[2]	IRBP source[2]
Soricomys montanus	DSB 4529	FMNH 193520	this study	
Soricomys montanus	LRH 7463	FMNH 188319	this study	
Soricomys montanus	DSB 3787	FMNH 188313	this study	
Soricomys kalinga	LRH 6436A	FMNH 170967	this study	
Soricomys kalinga	LRH 5946	FMNH 167304	this study	
Soricomys kalinga	EAR 5037	FMNH 175558	this study	
Soricomys musseri	DSB 3711	FMNH 185909	this study	
Soricomys musseri	DSB 3747	FMNH 185910	this study	
Soricomys musseri	PAA 609	FMNH 185907	this study	this study
Soricomys musseri	DSB 3704	FMNH 185908	this study	
Soricomys leonardocoi	PAA 818	FMNH 190974	this study	
Soricomys leonardocoi	DSB 4256	FMNH 190982	this study	this study
Soricomys leonardocoi	DSB 4155	FMNH 190970	this study	
Soricomys leonardocoi	DSB 4122	FMNH 190963	this study	
Apomys gracilirostris		CMNH M648	AY324466[6]	
Apomys musculus		USNM 458925	AY324482[6]	DQ191494[4]
Apomys microdon		FMNH 167242	AY324479[6]	DQ191493[4]
Apomys insignis		FMNH 147911	AY324470[6]	DQ191492[4]
Apomys hylocoetes		FMNH 147914	AY324468[6]	
Apomys camiguinensis		FMNH 154816	AY324476[6]	
Apomys datae		FMNH 167358	AY324464[6]	EU349836[5]
Phloeomys cumingi		USNM 573332	DQ191484[4]	AY326103[7]
Batomys granti		USNM 458914		DQ191496[4]
Batomys granti		USNM 458948	AY324459[6]	

[1] Collector number is used as the DNA number.
[2] Accession number is listed if sequence was downloaded from Genbank. Blank cells indicate sequences not included in this study.
[3] from Rickart et al. 2005.
[4] from Jansa et al. 2006.
[5] from Rowe et al. 2008.
[6] from Steppan et al. 2003.
[7] from Jansa and Weksler 2004.

EMENDED DIAGNOSIS: The genus *Archboldomys* is defined phylogenetically as the most recent common ancestor of *A. luzonensis* and *A. maximus* and all of its descendants (figs. 7, 8). They are small-bodied shrew mice most similar superficially to *Soricomys*, new genus, but differ from it and other known murids in the combination of the following cranial and dental features (table 11): (1) uniformly dark and unpatterned pelage; (2) tail substantially or slightly shorter than the length of head and body; (3) moderately long, tapered rostrum; (4) upturned nasal tips projecting slightly beyond the anterior margins of the premaxillae; (5) slanting anterior edge of zygomatic

FIG. 10. Skulls of **A,** *Archboldomys luzonensis* (FMNH 95122, holotype); **B,** *Soricomys musseri* (FMNH 147176, holotype); and **C,** *S. kalinga* (FMNH 175555, holotype). Modified from Balete et al. (2006).

TABLE 9. Parameter estimates under the best-fitting substitution model for each gene.

	Cytochrome *b*	IRBP
Model	GTR+I+Γ_4	HKY+Γ_4
πA	0.34	0.22
πC	0.34	0.28
πG	0.10	0.28
πT	0.22	0.22
TI/TV	NA	3.175
rAC	1.98	NA
rAG	10.19	NA
rAT	2.82	NA
rCG	0.08	NA
rCT	33.56	NA
α	0.17	0.22
pinv	0.004	0
ln-likelihood	-8261.37	-2862.01

TABLE 10. Results of model-fitting for the combined-gene dataset.

Partitioning scheme	Taxa (no.)	Characters (no.)	Parameters (no.)	HML[a]	AIC[b] Score	BIC[c] Score
Unpartitioned	19	2377	12	-9893.78	19811.68	20152.90
By gene	19	2377	20	-9585.50	19211.35	19598.54
By codon	19	2377	32	-9505.80	19076.50	19532.43
By gene by codon	19	2377	36	-9061.00	18195.14	18673.93

[a]Harmonic mean log-likelihood.
[b]Akaike information criterion.
[c]Bayesian information criterion.

plate relative to horizontal molar row; (6) long and slender tympanic hook; (7) spacious squamoso-mastoid vacuity; (8) mastoid entire or without fenestra in adults; (9) ophistodont upper incisor procumbency; (10) upper incisors forming an acute triangle at their posterior margin in ventral view (fig. 9); (11) broad molariform tooth row with prominent cusps (figs. 10, 11); (12) squarish first upper molars (figs. 10, 11); and (13) small but conspicuous interpremaxillary foramen present (fig. 9).

COMMENTS: *Archboldomys* and *Crunomys:* Musser (1982a) noted the similarity of *Archboldomys* to *Crunomys*, specifically *C. melanius* and *C. celebensis*, and hinted at a possibly close phylogenetic relationship, based in particular on the shape, simplified cuspidation, and occlusal patterns of their molars. He proposed the hypothesis that "the old native rodents of the Philippine Islands may represent an adaptive radiation in which all members are more closely related to each other than to rats and

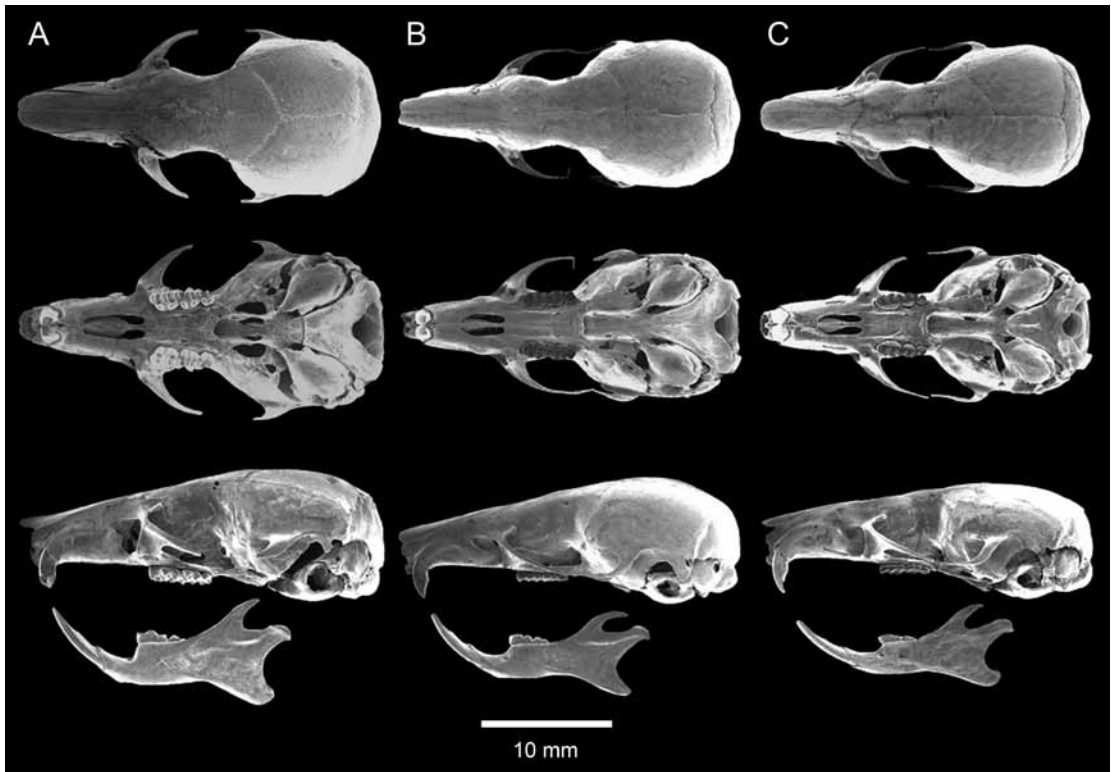FIG. 11. Upper molar rows of **A,** *Archboldomys luzonensis* (FMNH 95122, holotype); **B,** *Soricomys mussseri* (FMNH 147176, holotype); and **C,** *S. kalinga* (FMNH 175555, holotype). Modified from Balete et al. (2006).

mice on the Asian mainland to the west, Sulawesi and the Lesser Sundas to the south, or to Australia and New Guinea area to the east." In spite of including one species from Sulawesi (*C. celebensis*), *Crunomys* was grouped with *Archboldomys*, *Chrotomys*, *Celaenomys* (now part of *Chrotomys*; Rickart et al., 2005), and *Rhynchomys*. This was further reinforced in the first assessment of phylogenetic alliances of the native Philippine murid fauna (Musser and Heaney, 1992), in which the *Crunomys* Group was erected within the Old Endemic Division (Division I), consisting of *A. luzonensis*, *Crunomys fallax*, *C. melanius*, and *C. rabori* (now part of *C. melanius*; see Rickart et al., 1998).

TABLE 11. Distribution of primary characters that distinguish members of the *Chrotomys* Division of Philippine murid rodents.

Feature	Genus				
	Apomys	*Archboldomys*	*Chrotomys*	*Rhynchomys*	*Soricomys*
Color pattern	absent (except dorsal-ventral countershading)	absent	mid-dorsal stripe (only fore-head blaze or shoulder stripe in some *C. silaceus*)	absent (except dorsal-ventral countershading)	absent (except dorsal-ventral countershading)
Tail length relative to head and body length	slightly shorter to longer	shorter to slightly longer	shorter	shorter	shorter to slightly longer
Nasal tip extension relative to anterior margin of premaxillary	along edge	beyond edge	behind edge	beyond edge	along edge
Incisive foramina	long and broad	long and narrow	short and broad	long and narrow	short and broad
Interpremaxillary foramen	minute	short and narrow	long and wide	long and narrow	minute
Orientation of zygomatic plate	slanting	slanting	vertical	slanting	vertical
M1 relative to ventral maxillary root of zygomatic plate	overlap up to first row	overlap up to 2nd row	no overlap	complete overlap	overlap up to first row
Maxillary molar tooth row composition	complete	complete	complete (M3 absent in *C. silaceus*)	M3 absent	complete
Maxillary molar tooth row shape	long and narrow	long and broad	short and narrow	short and narrow	long and narrow
M1 and M2 shape	long and narrow	short and broad	short and narrow	short and narrow	long and narrow

Feature	Genus				
	Apomys	*Archboldomys*	*Chrotomys*	*Rhynchomys*	*Soricomys*
M3 size relative to M1 and M2	small	small	small (absent in *C. silaceus*)	absent	small
Upper incisors procumbency	orthodont	ophistodont	proodont	orthodont	orthodont
Posterior edge of upper incisors	rounded	acutely angular	broadly angular	acutely angular	broadly angular
Enamel coloration of upper incisors	orange	pale yellow-orange	pale yellow-orange	unpigmented	orange
Otic capsule attachment to cranium	absent	absent	present (absent in *C. silaceus*)	absent	absent
Tympanic hook shape	short and broad	long and narrow	short and broad	short and broad	short and broad
Squamoso-mastoid foramen	present	present (wide)	absent (present in *C. silaceus*)	absent	present (narrow)
Pterygoid ridge	present	present	absent	present	present
Pterygoid bridge	present	present	present	absent	present
Alisphenoid strut	present	present	present	absent	present
Mastoid fenestra	absent	absent	absent	absent	present
Mastoid foramen	absent	present	present	present	present
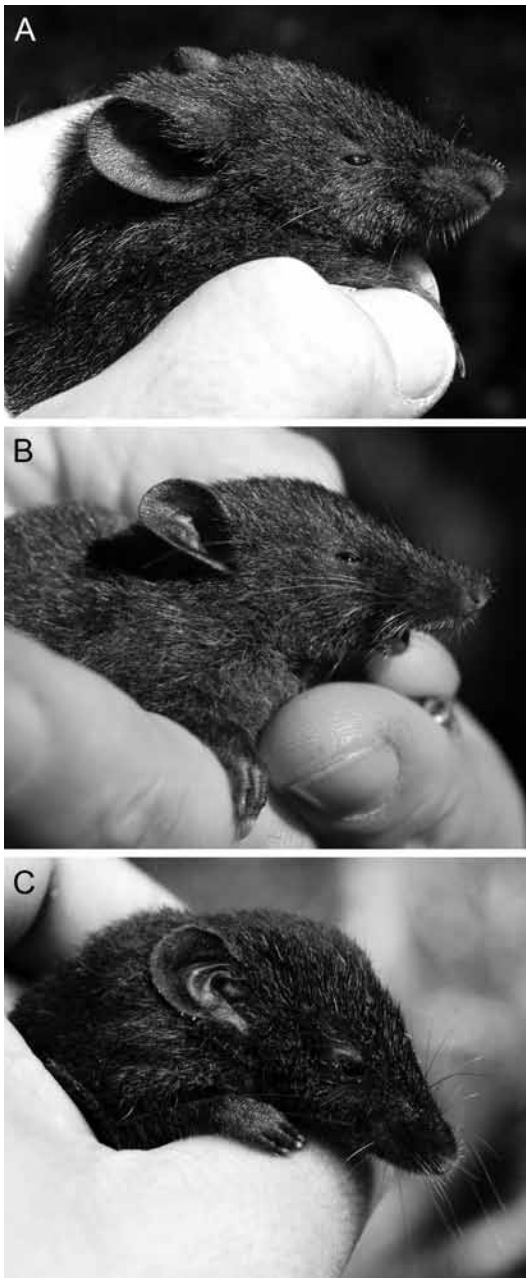
FIG. 12. **A,** *Archboldomys maximus* (FMNH 193525), adult female. Photographed by L.R. Heaney, 1 March 2007. **B,** *Soricomys montanus* (FMNH 193514), adult male. Photographed by J.F. Barcelona, 28 February 2007. **C,** *Soricomys leonardocoi* (FMNH 190962), adult male. Photographed by M.R.M. Duya, 29 May 2006.

The discovery of *Crunomys suncoides* on Mt. Kitanglad (central Mindanao) and *Soricomys musseri* (as *Archboldomys musseri*) on Mt. Cetaceo (NE Luzon) enabled further assessment of the hypothesized *Archboldomys-Crunomys* phylogenetic alliance and redefinition of both genera (Rickart et al., 1998). However, no shared derived morphological traits were found that unite *Archboldomy* and *Crunomys* as a distinct clade; the presumed synapomorphies in the shape, size, and simplified cuspidation patterns of molars of the two genera were inferred to have resulted from convergence on shrewlike feeding habits (Rickart et al., 1998). The karyotypic differences between *Archboldomys* and *Crunomys* (table 7; Rickart and Heaney, 2002), as well as additional cranial, dental, and external morphological differences, reinforced the hypothesized close phylogenetic link among *Archboldomys*, *Chrotomys*, and *Rhynchomys*, but were unsupportive of their sister-taxon relationship with *Crunomys* (Rickart and Musser, 1993; Rickart et al., 1998). The split between *Archboldomys* and *Crunomys* was later strongly supported by molecular data, indicating that *A. luzonensis* is closest to the members of the *Chrotomys* Division that includes *Rhynchomys*, *Chrotomys*, and *Apomys* (Jansa et al., 2006). *Crunomys* (represented by *C. melanius*), on the other hand, was recovered as sister taxon to *Maxomys*, within the clade that includes the Philippine native murid rodents belonging to the New Endemic Division, along with allied species from the Sunda Shelf (Musser and Heaney, 1992; Jansa et al., 2006).

Comparison of *Archboldomys* and *Soricomys*, new genus: Aside from *A. luzonensis*, shrew mice previously attributed to *Archboldomys* included *S. musseri* (as *A. musseri*) and *S. kalinga* (as *A. kalinga*), from Mt. Cetaceo in the Sierra Madre, and the vicinity of Mt. Bali-

it in Kalinga Province, in the northern Central Cordillera, respectively (fig. 1; Musser, 1982a; Rickart et al., 1998; Balete et al., 2006). Some additional specimens from the southern Central Cordillera were referred to "*A.*" *kalinga* (Heaney et al., 2010; Rickart et al., 2011b). They were discussed within the context of broadening morphological and geographical ranges of the genus *Archboldomys*, but a suite of diagnostic features that set apart the two species groups (i.e., *A. luzonensis* vs. the other two) was highlighted in the description of the latter two species (see the diagnosis of *Soricomys*; Rickart et al., 1998; Balete et al., 2006). We confirmed the consistency of the differences with the collection of a large, short-tailed species in the Central Cordillera (*A. maximus*, n. sp.) that occurred sympatrically with the small, relatively long-tailed *S. montanus,* n. sp., on Mt. Amuyao (fig. 1). These discoveries clearly indicated the presence of two species groups of shrew mice on Luzon, consisting of a relatively larger-bodied, short-tailed group composed of *A. luzonensis* and *A. maximus*, n. sp., from Mt. Amuyao, and a smaller-bodied, relatively longer-tailed group composed of *S. kalinga*, *S. musseri, S. leonardocoi,* n. sp., and *S. montanus,* n. sp. (fig. 12). The two groups are separated by distinct and consistent differences in

FIG. 13. Cranium and mandible of *Archboldomys maximus,* adult male (FMNH 193531, holotype) in dorsal, ventral, and lateral views.

external, cranial, and dental features; among the most prominent differences (for *Archboldomys* vs. *Soricomys*) are longer incisive foramina (vs. shorter); small but apparent interpremaxillary foramena (vs. absent, with only tiny nutrient foramina present); zygomatic plate slanting (vs. nearly perpendicular to molar row); M1 and M2 short and broad (vs. long and narrow); upper incisors slightly [*A. luzonensis*] to strongly [*A. maximus,* n. sp.] ophistodont (vs. orthodont); upper incisors forming an acute angle at posterior tips in ventral view (vs. broadly rounded; fig. 9); and tympanic hook long and narrow (vs. short and broad; figs. 3, 10, 13; tables 1–5, 11). Both *Archboldomys* and *Soricomys,* n. gen., have the carotid arterial pattern in which a large stapedial artery branches off from the common carotid artery and enters the otic capsule through the stapedial foramen, passes through the bulla, and then passes through a groove in the pterygoid plate into the foramen ovale (see Musser, 1982a: figs. 30, 31).

This distinction between *Archboldomys* and *Soricomys* is also supported by the karyotypic data showing substantial differentiation between *Archboldomys* and *Soricomys,* new genus, especially in diploid number and X-chromosome morphology (table 7; fig. 5; Rickart and Heaney, 2002). Our phylogenetic analyses of molecular data from representatives of these species and other members of the *Chrotomys* Division (*Apomys*, *Chrotomys*, and *Rhynchomys*) not only supported the above morphological and karyological differentiation between the two groups, it also failed to recover the monophyly of *Archboldomys*. Instead, it showed that the small-bodied members (*Soricomys,* n. gen.) are the sister taxon to *Chrotomys*, and the large-bodied members (*Archboldomys* sensu stricto) are sister to the clade that includes *Soricomys*, *Chrotomys*, and *Rhynchomys* (figs. 7, 8). This evidence clearly supports the establishment of a new genus, *Soricomys*, that accommodates two shrew mice formerly attributed to *Archboldomys* (*S. kalinga* and *S. musseri*), and two additional new species, as described below.

Archboldomys luzonensis Musser, 1982

HOLOTYPE: FMNH 95122. Young adult male collected on 24 April 1961, field number D.S. Rabor 1149 (Musser, 1982a: figs. 13, 22–32). Prepared as stuffed skin with skull (fig. 10A) removed and cleaned.

TYPE LOCALITY: Philippines: Luzon Island: Camarines Sur Province: Mt. Isarog, 6560 feet.

MEASUREMENTS: Tables 1 and 2.

SPECIMENS EXAMINED (*N* = 14): Camarines Sur Province, Mt. Isarog National Park, 1350–1750 m (FMNH 147172, 147173, USNM 573505, 573834–573840, PNM 4683); 4 km N, 21.5 km E Naga City, 1550 m (FMNH 152031, 152032); Pili Municipality, Mt. Isarog, 6560 ft (FMNH 95122 [holotype]).

EMENDED DIAGNOSIS: A shrew mouse of the genus *Archboldomys*, readily distinguished from *A. maximus*, n. sp., by the following combination of external, cranial, and dental features: (1) smaller body; (2) shorter, reddish-brown pelage; (3) absolutely and relatively shorter tail, with fewer scale rows (TSR); (4) absolutely and relatively shorter hind foot; (5) shorter and narrower skull; (6) longer incisive foramina; (7) larger (though short and broad) interpremaxillary foramen; (8) wider zygomatic plate; (9) greater orbito-temporal length; (10) shorter and narrower pterygoid ridge, terminating posteriad below the alisphenoid strut; (11) broader and conspicuously exposed alisphenoid strut (see Musser, 1982a: fig. 23A); (12) slightly more elongate and narrowly angled posterior edge of upper incisors; (13) narrower and shorter maxillary and mandibular molar rows; (14) smaller molars in which cusp t3 and t9 are either missing from M1 or so broadly merged with the adjacent cusp in the respective cusp row that they are unidentifiable; (15) shorter and broader mandible; (16) broader angular process; and (17) longer and more robust coronoid process (figs. 10A, 13; table 11).

KARYOLOGY: 2N = 26 and FN = 43 (fig. 6A; Rickart and Musser, 1993; Rickart and Heaney, 2002).

COMPARISONS: See Description and Comparisons section of *A. maximus*, below.

DISTRIBUTION: Known only from Mt. Isarog, southeastern Luzon Island (Rickart et al., 1991; Balete and Heaney, 1997; Heaney et al., 1999).

Ecology: *Archboldomys luzonensis* is a montane and mossy forest specialist, occurring at 1350 m to 1750 m; it was not recorded below 1350 m (Rickart et al., 1991; Balete and Heaney, 1997; Heaney et al., 1999). Laurels, myrtles, oaks, and podocarps were the common canopy and emergent trees in these forests, often reaching a canopy height of ca. 12–20 m in montane forest, and 5–12 m in mossy forest. Moss cover ranged from moderate in montane forest, to covering most surfaces of trees and ground in mossy forest; leaf litter in both habitats was extensive, and the humus layer was thick. Vegetation of these habitats was described in more detail in Heaney et al. (1999).

The morphological adaptations of *A. luzonensis* (e.g., small, robust body with short tail, short limbs, and small ears, short dense pelage, and long, sharp claws) suggest a semifossorial habit. It is active during the day, possibly extending from dawn to dusk; in 1988, seven of eight individuals captured were taken during the day and the eighth near dawn (Heaney et al., 1999). They were captured mostly along runways under root tangles, under fallen logs, or beside ground vegetation. In 1993–1994, two individuals were observed foraging in leaf litter in mossy forest during the day (Balete and Heaney, 1997). Stomach contents, consisting of amphipods, larval and adult arthropods, and earthworms, suggest a vermivorous/insectivorous diet (Heaney et al., 1999). Earthworms were abundant where this species was captured (Rickart et al., 1991). Females have two pairs of inguinal mammae. Two pregnant females, recorded in late March and late April, each had a single embryo (Heaney et al., 1999). The species appeared to be moderately common in mossy forest on Mt. Isarog, with an estimated density of ca. 4.5 ± 1.63 individuals/ha (Balete and Heaney, 1997).

Other nonvolant small mammals recorded along with *Archboldomys luzonensis* in montane and mossy forest included *Crocidura grayi*, *Apomys microdon*, *A. musculus*, *Batomys* cf. *granti*, *Chrotomys gonzalesi*, *Phloeomys cumingi*, *Rattus everetti*, and *Rhynchomys isarogensis* (Balete and Heaney, 1997; Heaney et al., 1999; Rickart et al., 1991). Of these, five are members of the *Chrotomys* Division: *A. microdon*, *A. musculus*, *C. gonzalesi*, and *R. isarogensis* (table 12).

Archboldomys maximus, new species
Figures 8B, 11A, 12, 13

Holotype: FMNH 193531. Adult male collected on 23 March 2007, field number D.S. Balete 4560. Fresh tissues were removed from the thigh and placed in 95% ethanol. The rest of the specimen was initially fixed in formalin, now preserved in ethyl alcohol with skull (fig. 13) removed and cleaned. The holotype is currently housed at FMNH but will be transferred to PNM.

Type Locality: Philippines: Luzon Island: Mountain Province: Barlig Municipality: 1.75 km N, 0.4 km W Mt. Amuyao peak, 1885 m elevation, 17.02929° N, 121.12466° E (fig. 1).

Measurements: Tables 1 and 2.

Specimens Examined (N = 13): Mountain Province, Barlig Municipality, Mt. Amuyao peak, 2690 m (FMNH 193524); 0.5 km N, 0.5 km W Mt. Amuyao peak, 2530 m (FMNH 193522, 193523); 0.4 km N, 0.4 km W Mt. Amuyao peak, 2480 m (FMNH 193525–193527); 0.75 km W Mt. Amuyao peak, 2300 m (FMNH 193528, 193942, 193943); 1.0 km N, 1.0 km W Mt. Amuyao peak, 2150 m (FMNH 193529, 193530); 1.75 km N, 0.4 km W Mt. Amuyao peak, 1885 m (193531 [holotype], 193944).

ETYMOLOGY: From the superlative of *magnus* (Latin: "great, large"), to highlight its being the largest of the seven species of shrew mice (*Archboldomys*, *Crunomys*, and *Soricomys*) on Luzon. We recommend as the English common name either "large Cordillera shrew mouse" or "Cordillera archboldomys."

DIAGNOSIS: *Archboldomys maximus* is a shrew mouse similar to *A. luzonensis,* but readily defined by the following combination of external, cranial, and dental characters and proportions (tables 1, 2, figs. 9–14): (1) long, robust body; (2) dark chestnut pelage; (3) tail nearly as long as head and body, with fine scale rows; (4) relatively long hind feet; (5) long, broadly ovate skull with tapered rostrum and more strongly inflated cranium; (6) proportionately short incisive foramina; (7) interpremaxillary foramen small and slightly elongate, visibly posterior to line connecting the posterior edges of incisors (fig. 9); (8) narrow zygomatic plate with pronounced slanting anterior edge; (9) short orbito-temporal length; (10) long and wide pterygoid ridge extending posteriad to become the pterygoid bridge over the foramen ovale; (11) narrow and delicate alisphenoid strut; (12) narrow, sharply angled posterior edge of upper incisors (fig. 9); (13) long molariform tooth row; (14) large molars with complete cuspidation on the first molar (cusps t3 and t9 clearly present but broadly merged with adjacent cusps; cusp t8 with anterolingual projection); (15) long and narrow mandible; (16) narrow angular process; and (17) short and narrow coronoid process.

DESCRIPTION AND COMPARISONS: *Archboldomys maximus* is the larger of the two species of *Archboldomys*, and is readily distinguishable externally from *A. luzonensis* by its longer and more robust body overall (smaller, shorter body in *A. luzonensis*); dark grayish chestnut pelage (reddish brown); absolutely and relatively longer tail, with finer scale rows (absolutely and relatively shorter tail, with larger and fewer scale rows); longer, broader, and more darkly pigmented hind feet (shorter, narrower, and paler hind feet) (fig. 12, table 1; Musser, 1982a: fig. 22).

The pelage of *A. maximus* is uniformly grayish chestnut, longer and thicker dorsally than ventrally. The rostrum is tapered and the face is broad (fig. 12A). The pale grayish-brown vibrissae extend slightly beyond the ears. The lips and rhinarium are pigmented pale grayish brown. The eyelids are finely edged with dark gray, surrounded by a narrow paler band covered with short dark grayish-brown fur. The ears are small, round, medium grayish brown, and covered with short black hairs.

The front feet of *A. maximus* are small, with relatively short, robust digits bearing long, opaque claws with decurved tips, except the pollex, which is short and bears a nail. The dorsal and palmar surfaces are uniformly pigmented dark grayish brown. The palmar pads consist of three interdigitals, and a thenar and hypothenar, which are larger than the interdigitals. The hind feet are long and slender, with relatively short digits; the longest middle digits including claws are less than one-third the length of the hind foot. The claws are opaque, shorter than on the forefeet and with short decurved tips. Both the dorsal and plantar surfaces, including digits and plantar pads, are pigmented dark grayish brown. The plantar pads are small relative to plantar surface and consist of four interdigitals, a large thenar, and smaller, round hypothenar; the metatarsal is small and rounded; the rest are ovate and larger.

The tail of the holotype of *A. maximus* is 13% shorter than the combined length of head and body; the paratypes have from 20% shorter to slightly longer tail than the combined length of head and body (table 1). There are ca. 20 tail scale rows/cm (TSR) in the holotype, 20–24 TSR in paratypes; each scale bears three short hairs. Tail is uniformly pigmented dark grayish brown, with its dorsal surface covered with short, similarly pigmented hairs and its ventral surface covered with a mix of dark and pale to unpigmented hairs.

Archboldomys maximus and *A. luzonensis* have similarly upturned nasal tips that project beyond the anterior margins of the premaxillae and broad, squarish first molars, and upper incisors with acutely angled posterior edges (figs. 9, 10, 13). However, differences in cranial features and measurements easily distinguish *A. maximus* from *A. luzonensis* (tables 2, 11; figs. 9–13; Musser, 1982a: figs. 13; 22–24, 26–30; Rickart et al., 1998: fig. 12), including: (1) a longer, broadly ovate skull with proportionately longer rostrum (shorter in *A. luzonensis*) and laterally inflated braincase (less inflated); (2) shorter incisive foramina (longer); (3) elongate interpremaxillary fossa that is placed well behind a line connecting the posterior margins of the incisors (rounded interpremaxillary foramen, close to a line connecting the posterior margins of the incisors); (4) narrow zygomatic plate with a more pronounced slanting anterior edge (wider and less slanting); (5) shorter orbito-temporal length (longer); (6) longer and wider pterygoid ridge extending posteriad to become the pterygoid bridge over the foramen ovale (shorter and narrower, terminating posteriad above alisphenoid strut); (7) and narrow, delicate alisphenoid strut hidden under pterygoid ridge (broad, robust, and conspicuously exposed alisphenoid).

The skull of *A. maximus* is smooth, with gracile, tapered rostrum and dorsolaterally swollen cranium (figs. 3, 9, 13). In lateral view, its dorsal profile is nearly straight from the top of the skull to about the anterior base of the premaxilla, from which the profile assumes a short and smoothly shallow anteriad convexity brought about by the upturned nasal tips. The nasal tip projects beyond the anterior edge of the premaxillae. The slightly raised bony capsule of the upper incisor root terminates medially near the suture with the maxilla, opposite the dorsal opening of the small and narrow lachrymal canal. The opening of this canal slants caudad, and its nearly flat outer wall barely projects beyond the lateral outline of the capsular swelling of the upper incisor root. The zygomatic plate slants dorsad, relative to the upper molar tooth row. The zygomatic process of the squamosal is low on the cranium, anchored less than a millimeter above the dorsal edge of the postglenoid foramen.

The tympanic hook of the squamosal is slender and short relative to cranial size. The squamoso-mastoid foramen is small relative to the postglenoid vacuity and is either obscured entirely by a thin membrane, as in the holotype, or partially obscured ventrally by the wide, posterior extension of the periotic part of the petromastoid. The mastoid of adults has no fenestra (e.g., FMNH 193526, 193943, 193944). In younger adults, a narrow slit in various stages of closure is present in the mastoid (as in the left mastoid of the holotype [the right one is completely ossified], FMNH 193531; fig. 13). A small mastoid foramen is situated along the medial occipital suture.

The incisive foramina of *A. maximus* are long and narrow, round edged posteriad and smoothly tapered anteriad (fig. 13, table 2). A small interpremaxillary foramen is present, lying visibly posterior to a line connecting the posterior edges of the incisors (fig. 9). The alisphenoid

canal is small and circular, bridged by the thin alisphenoid strut, both well concealed under the wide pterygoid ridge. The pterygoid ridge itself is also long, extending posteriad and becoming the pterygoid bridge over the foramen ovale. The postglenoid vacuity is spacious and domed, and the widest part appears nearly round due to the smooth concavity of the posterior periotic part of the petromastoid opposite the domed dorsal edge; in the holotype, the left vacuity is sealed by a membranous covering. The auditory bulla is small relative to cranial area, and anteroventrally inflated (viewed right side up), obscuring the anterior half of the petrosal in ventral view.

Dental features are strikingly similar between *A. maximus* and *A. luzonensis*, both sharing slightly (*A. luzonensis*) or strongly (*A. maximus*) ophistodont upper incisor procumbency, upper incisors in ventral view that are sharply angled on the posterior edge (fig. 9), and squarish first upper molars. But several dental and mandibular features and measurements easily distinguish *A. maximus* from *A. luzonensis* (figs. 2, 3, 9–14, table 2; Musser, 1982a: figs. 13, 32, 33; Rickart et al., 1998: fig. 12), including longer molariform tooth row (shorter in *A. luzonensis*), larger molars with complete cuspidation on the first upper molar (fig. 2; smaller, with absent or missing cusp t3 and cusp t9 on M1), longer and more gracile mandible (shorter and more robust), narrow angular process (wider), and shorter and narrower coronoid process (longer and wider).

The maxillary molars of *A. maximus* (figs. 2, 14) are marked by their large size. The first upper molar appears squarish due to the conspicuous broadening of the lingual cusps t1 and t4 that together contribute to the width of M1, which is about three-fourths of its length. The cuspidation of the three rows of M1 appears complete (fig. 2), though coalesced in the broad laminar outlines of the deeply basined occlusal surface, cusp t3 on the first row is barely visible at the edge of the worn, broad, and downsloping labial lamina, and cusps t7 and t9 have either merged with t8 or are absent. The second molars are smaller than the first, but the anterolingual convexity of cusps t1 and t4 makes them wider than long, and trapezoidal in occlusal outline. Cusps t2 and t3 are missing on the first row. The second and third rows appear to have complete cuspidation, coalesced in the laminar outlines of their occlusal surfaces. The third molar has less than half the surface area of the second molar, and has a cordate occlusal outline brought about by the broad lingual cusp t1 and what appears to be the anterolabially oriented second row, with presumed cusps t4, t5, and t6 coalesced into the narrow laminar outline of its occlusal surface. The slanting orientation of this second row results in posteriad placement of cusp t4 (figs. 2, 14). No evidence of a third row is discernible.

The dentary of *A. maximus* is slightly longer and more gracile than in *A. luzonensis* (figs. 10, 13; Musser, 1982a: fig. 13). The labial surface of the mandible is smooth, and the capsular process is barely discernible. The placement of the mandibular and mental foramina is similar to *A. luzonensis*. The mandibular molar row (fig. 14B) is slender. The lower incisors are robust, sharply pointed, and the anterior surface covered with pale yellow enamel (fig. 13). The incisor is broadly procumbent, forming a smooth, wide curve from the anterior edge of the first mandibular molar alveolus. The coronoid process is short, slender, and backswept, extending slightly more than halfway from its base to the base of the adjacent condyle. The condyloid process is short and robust. The angular process is slender with a narrowly angular and slightly upturned tip, forming a deep sigmoidal notch with the posterior edge of the condyle.
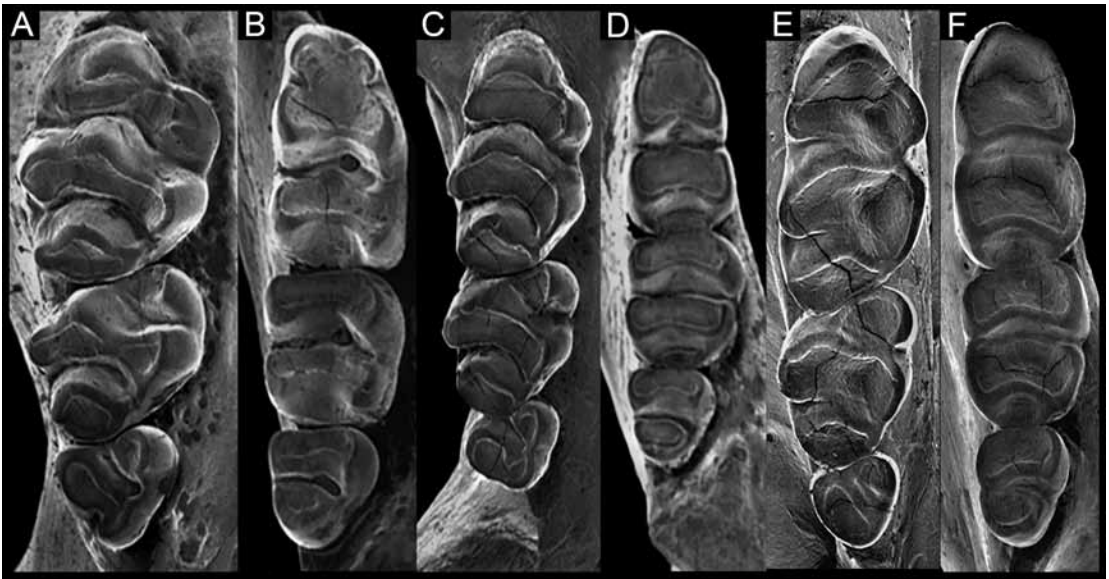
FIG. 14. Occlusal view of maxillary and mandibular molar toothrows of **A–B,** *Archboldomys maximus* (FMNH 193531, holotype), **C–D,** *Soricomys leonardocoi* (FMNH 190972, holotype), and **E–F,** *Soricomys montanus* (FMNH 188314, holotype).

As noted above, a PCA analysis based on cranial and dental measurements (fig. 4, table 5) demonstrated no overlap between *A. luzonensis* and *A. maximus* on the second axis, with *A. maximus* having a proportionally longer skull, more elongate diastema and postpalatal region, and broader upper incisors measured near the tips, and *A. luzonensis* having the converse. Analysis of the mitochondrial cytochrome *b* and IRBP nuclear gene gave strong support to these two species as sister taxa, with branch lengths separating them similar to those separating the species of *Soricomys* (figs. 7, 8).

Distribution: Currently known only from Mt. Amuyao, Mountain Province, in the Central Cordillera of northern Luzon (figs. 1, 15; Rickart et al., 2011b). However, Mt. Amuyao is the only place in the southern portion of the Central Cordillera where surveys in the relevant habitat (mature montane and mossy forest) using the relevant sampling methods (traps baited with live earthworms) have been conducted. The species may occur in montane and mossy forest over a broad portion of the Central Cordillera; additional surveys are needed to determine the extent of its distribution.

Ecology: *Archboldomys maximus* has been captured in old-growth montane and mossy forest, from 1885 m to 2690 m (Rickart et al., 2011b). There were slightly more diurnal (8) than nocturnal/crepuscular (5) captures. Success with traps baited with live earthworms was higher than with fried coconut, but the effect was not statistically significant. Stomach analysis suggests a predominantly vermivorous feeding habit; stomach contents of six individuals all included earthworms, in addition to centipedes (order Geophilomorpha) in three individuals, and a few fragments of insect exoskeletons (body and integument of adults and larvae) in four individuals.

Females have two pairs of mammae, both inguinal. Reproductive activity early in the year was apparent. Five of six males caught in March had scrotal testes, one of which had a testes size of 10×7 mm with convoluted epididimys; during the same period, two of seven females had large mammae, one of which was pregnant with a single embryo and had one placental scar (Balete, Heaney, and Rickart field notes in FMNH).

Eleven other species of nonvolant small mammals were recorded in montane and mossy forest habitat with *Archboldomys maximus*: *Crocidura grayi*, *Apomys datae*, *A. musculus*, *Batomys granti*, *Bullimus luzonicus*, *Chrotomys silaceus*, *C. whiteheadi*, *Musseromys* sp., *Rattus everetti*, *Rhynchomys soricoides*, and *Soricomys montanus,* new species (Rickart et al., 2011b). Among them, six are members of the *Chrotomys* Division: *Apomys datae*, *A. musculus*, *S. kalinga*, *C. silaceus*, *C. whiteheadi*, and *R. soricoides* (table 12). Mt. Amuyao is the only place known currently where species of *Archboldomys* and *Soricomys,* n. gen., occur sympatrically. Additional species of native nonvolant mammals we documented on Mt. Amuyao included *Apomys abrae* (at lower elevations), and the giant cloud rats *Crateromys schadenbergi* and *Phloeomys pallidus* (Rickart et al., 2011b).

Soricomys, new genus

Type Species: *Archboldomys kalinga* (Balete, Rickart, and Heaney, 2006).

Etymology: From the Latin *sori-* (*sorex*, "shrew"), in combination with *mys* (Gk., "mouse"), for its close similarity to the shrews in body form and habits. Gender masculine.

Included Species: As currently understood, *S. kalinga*, *S. leonardocoi*, n. sp., *S. montanus*, n. sp., and *S. musseri*. See comments below.

Distribution: Luzon Island only; currently known only from the Central Cordillera, the Mingan Mountains, and the northern Sierra Madre (fig. 1).

Diagnosis: A genus of small-bodied shrew mice, superficially similar to *Archboldomys* in external morphology, but distinguished from it and other known murid rodents by the following combination of external, cranial, and dental features (table 11): (1) dorsal fur darker and longer than ventral fur; (2) short, tapered rostrum; (3) straight nasal tips terminating above the anterior margins of the premaxillae; (4) straight anterior edge of zygomatic plate relative to the horizontal molar row; (5) short and broad tympanic hook; (6) narrow to nearly closed squamoso-mastoid foramen; (7) prominent mastoid fenestra; (8) orthodont upper incisors procumbent; (9) broadly angled to nearly rounded lingual edge of upper incisors; (10) narrow molar row; (11) relatively narrow, rectangular upper first molars, M1; and (12) interpremaxillary foramina (and presumably the vessel it transmits) absent (only minute nutrient foramina present; fig. 9).

Comments: Comparisons to *Archboldomys* are given above.

Soricomys kalinga (Balete et al., 2006) and *S. musseri* (Rickart et al., 1998) were both originally described as members of *Archboldomys*. Several cranial and dental characters highlighted during the original diagnosis of *S. musseri,* including straight nasal tips, short incisive foramina, small postglenoid vacuities, prominent mastoid fenestra, and smaller molars, are now among the diagnostic features of *Soricomys* (table 11). Also, as noted in the original description, the ventral pelage of *S. musseri* is slightly shorter and paler than the dorsal fur (with a gradual

TABLE 12. Distribution of members of the *Chrotomys* Division in sympatry with *Archboldomys* and *Soricomys* on Luzon Island.

Location of mountains indicated in figure 1. Except for *A. abrae* and *C. mindorensis*, species present on each mountain were recorded in the same habitat and elevation as with *Archboldomys* and *Soricomys*.

Species	Mountain and peak elevation (m)						
	Cetaceo 1657	Isarog 1966	Mingan 1901	Bali-it 2150	Data 2310	Amuyao 2702	Pulag 2922
Apomys microdon	X	X	X	X	X	X	X
Apomys musculus	X	X	X	X	X	X	X
Apomys abrae				X	X	X	
Apomys aurorae			X				
Apomys datae				X	X	X	X
Apomys minganensis			X				
Apomys sierrae	X						
Archboldomys luzonensis		X					
Archboldomys maximus						X	
Chrotomys gonzalesi		X					
Chrotomys mindorensis	X		X				
Chrotomys silaceus				X	X	X	X
Chrotomys whiteheadi				X	X	X	X
Rhynchomys isarogensis		X					
Rhynchomys soricoides				X	X	X	X
Rhynchomys sp.			X				
Soricomys kalinga				X			
Soricomys leonardocoi			X				
Soricomys montanus					X	X	X
Soricomys musseri	X						
Number of species	4	5	7	8	8	9	8

transition between them), in contrast to the uniformly colored pelage of *A. luzonensis*. The discovery of the three new species, *A. maximus, S. leonardocoi*, n. sp., and *S. montanus*, n. sp., demonstrates the consistency of these differences.

Phylogenetic analysis of mitochondrial cytochrome *b* and nuclear IRBP genes gave strong support to these four species as a clade, with an unresolved trichotomy among *S. musseri, S. leonardocoi*, n. sp., and a branch containing *S. kalinga* and *S. montanus*, n. sp. Although we do not advocate using threshold genetic divergence values as a way to diagnose species, we note that divergence values among species of *Soricomys* are comparable to or higher than those among other currently recognized species of this group. Notably, average uncorrected (p) sequence divergence for cytochrome *b* ranges from 7.9% to 8.9% among these four species of *Soricomys*, which

is similar to the divergence between the two species of *Archboldomys* (9.1%); within the range of divergence values among species of *Chrotomys* (2.8% to 11.7%); and much higher than the divergence values observed among recognized species of *Rhynchomys* (1.4% to 3.1%; fig. 7).

<div align="center">

Soricomys musseri (Rickart et al., 1998)
</div>

Archboldomys musseri Rickart, Heaney, Tabaranza, and Balete, 1998: 17.

Holotype: FMNH 147176. Adult male collected on 15 May 1992, field number D.S. Balete 2092 (figs. 10–11; Rickart et al., 1998: figs. 8–10). Initially fixed in formalin, now preserved in ethyl alcohol with skull removed and cleaned. Fresh tissues were removed from the thigh at the time of capture and placed in ethanol. The holotype is currently housed at the FMNH, but will be transferred to the PNM.

Type Locality: Philippines: Luzon Island: Cagayan Province: Peñablanca Municipality: Barangay Callao: Mt. Cetaceo, 1650 m elevation, 17°42´N, 122°02´E (fig. 1). See comments below.

Measurements: Tables 3 and 4.

Specimens Examined (*N* = 5): Cagayan Province, Peñablanca Municipality, Mt. Cetaceo, 1650 m (FMNH 147176 [holotype]); 1.5 km SW Mt. Cetaceo peak, 1550 m (FMNH 185907, 185910); 2.0 km SW Mt. Cetaceo peak, 1500 m (FMNH 185908, 185909).

Emended Diagnosis: A species of *Soricomys* distinguished from congeners by the following combination of characters: (1) dark, reddish-brown fur dorsally, shorter and paler ventrally; (2) absolutely and relatively shorter hind foot; (3) longer nasals; (4) dorsally inflated and higher cranium; (5) shorter and broader tympanic hook; (6) narrower squamoso-mastoid vacuity; (7) spacious postglenoid vacuity; (8) slender, backswept coronoid process; and (9) narrow, broadly angled angular process relative to condyle, and nearly straight-edged dorsally (figs. 9–11).

Comparisons: Externally most similar to *S. leonardocoi*, n. sp., but distinguished by the following combination of features (figs. 9–11, 13, 14, tables 3, 4, 11; Rickart et al., 1998: figs. 6–8, 12, 13): (1) absolutely and relatively shorter hind foot; (2) shorter, paler fur; (3) relatively longer tail; (4) narrower interorbit; (5) greater zygomatic breadth; (6) narrower zygomatic plate; (7) longer nasals; (8) shorter incisive foramina; (9) narrower squamoso-mastoid vacuity; (10) shorter maxillary molar tooth row; (11) narrower first upper molars, M1; and (12) broader incisors at their tips. Distinguished from *S. kalinga* by the following combination of features (figs. 9–11, tables 3, 4; Balete et al., 2006: figs. 4–6; Rickart et al., 1998: figs. 6–8, 12, 13): (1) relatively shorter tail; (2) absolutely and relatively shorter hind foot; (3) longer, darker fur; (4) dorsolaterally inflated cranium; (5) higher braincase; (6) broader interorbit; (7) wider zygomatic breadth; (8) longer nasals; (9) narrower squamoso-mastoid vacuity; (10) longer maxillary molar row; (11) wider palatal breadth at M1; and (12) wider labial breadth at M3. Distinguished from *S. montanus,* n. sp., by the following combination of features: (1) relatively shorter tail; (2) relatively shorter hind foot; (3) higher and dorsolaterally inflated cranium; (4) greater zygomatic breadth; (5) shorter and shallower rostrum; (6) longer nasals; (7) greater orbito-temporal length; (8) longer maxillary molar row (M1–M3); (9) wider palatal breadth at M1; (10) shorter diastema; (11) greater postpalatal length; (12) greater labial palatal breadth at M3; (13) wider incisors at their tips; (14) narrower zygomatic plate**.**

A PCA analysis of cranial and dental measurements (fig. 4, table 5) that included all species of *Archboldomys* and *Soricomys* (fig. 4, table 5) demonstrated clear separation of *S. musseri* from *Soricomys leonardocoi*, n. sp., on the second axis, with *S. kalinga*, *S. montanus*, n. sp., and *S. musseri* having a proportionately longer skull, more elongate diastema and postpalatal region, and broader upper incisors near their tips, and *S. leonardocoi*, n. sp., having the converse. *Soricomys musseri* differed from *S. kalinga* slightly on the first axis, an indication of its overall larger size. *Soricomys musseri* was most similar to *S. montanus*, n. sp., differing in scoring slightly higher on the first axis, indicating greater size. A PCA that included only the four species of *Soricomys* (fig. 5, table 6) produced similar results, with *S. musseri* loading less heavily on the first component and more heavily on the second component than *S. leonardocoi*, n. sp., indicating that *S. musseri* averages smaller overall and has shorter basioccipital length, rostral depth, rostral length, diastema length, and breadth of incisors near their tips. *Soricomys musseri* differed from *S. kalinga* and *S. montanus*, n. sp., in this PCA on the first component, which generally indicates its larger size.

Distribution: Currently known only from Mt. Cetaceo, in the northern Sierra Madre from 1500 m to 1650 m (figs. 1, 15; Duya et al., 2011). We hypothesize that it will be found north from Mt. Cetaceo (1730 m) to the Twin Peaks (peak at 1603 m) to at least as far south as Mt. Cresta (1672 m) in Isabela Province, and possibly from Mt. Palanan (1212 m) in southern Isabela Province to Mt. Anacuao (1853 m) in Aurora Province; these areas are typically (though intermittently) above 1500 m (fig. 15).

Ecology: *Soricomys musseri* has been documented in montane and mossy forest on Mt. Cetaceo, from 1500 m to 1650 m (Rickart et al., 1998; Duya et al., 2007, 2011). Based on trapping success, *S. musseri* appeared to be uncommon, with only four captures in 2395 ground-trap nights; the majority (75%, $N = 3$) were caught with earthworm bait, possibly indicating a vermivorous diet (Duya et al., 2011). Males with scrotal testes were captured in May and June; the two females, captured in June, were young adults with two pairs of small inguinal mammae. Also recorded in the montane and mossy forest habitat of *S. musseri* were two other members of the *Chrotomys* Division: *Apomys musculus* and *A. sierrae*; another member of the clade, *A. microdon*, was documented slightly lower on the mountain, at 1400 m (table 12). Other nonvolant small mammals recorded on the mountain included *Crocidura grayi*, *Bullimus luzonicus*, and *Rattus everetti* (Duya et al., 2011).

Comments: The attribution of the type locality in the original description to Callao Municipality was erroneous, as Callao is actually a *barangay* (a smaller political unit within a municipality), instead of Peñablanca, which is the correct name of the municipality. The first specimen, which later became the holotype of this species, was initially reported as *Crunomys fallax* (Danielsen et al., 1994).

Soricomys kalinga (Balete, Rickart, and Heaney, 2006)

Archboldomys kalinga Balete, Rickart, and Heaney, 2006: 491.

Holotype: FMNH 175555. Adult male collected on 23 February 2003, field number E.A. Rickart 5001 (figs. 9–11). Fresh tissues were removed from the thigh and placed in 95% ethanol. The rest of the specimen was initially fixed in formalin, now preserved in 70% ethyl alcohol

with skull removed and cleaned. The holotype is currently housed at FMNH, but will be transferred to PNM.

TYPE LOCALITY: Philippines: Luzon Island: Kalinga Province: Balbalan Municipality: Mt. Bali-it, 1950 m elevation, 17°25.8′N, 121°00.1′E (fig. 1).

MEASUREMENTS: Tables 3 and 4.

SPECIMENS EXAMINED (*N* = 22): Kalinga Province: Balbalan Municipality, Am-licao, 1800 m (FMNH 169122–169124, 170965–170967), Magdallao, 1600 m (FMNH 167304–167309), Mt. Bali-it, 1950 m (FMNH 175552–175555 [holotype], 175556), Mt. Bali-it, 2150 m (FMNH 175557–175559, 175720, 175721).

EMENDED DIAGNOSIS: A small shrew mouse of the genus *Soricomys*, distinguished from congeners by the following combination of features: (1) uniformly orange-brown dorsal pelage, shorter and paler on the venter; (2) narrow, dorsally flattened cranium; (3) long and slender tympanic hook; (4) deep rostrum; (5) long diastema; (6) narrow palate at M1; (7) short maxillary molar row; (8) short first upper molars; (9) robust, broadly backswept coronoid process; (10) robust, broadly tapered condyle; and (11) short, robust angular process (figs. 9–11).

KARYOLOGY: 2N = 44; FN unknown (fig. 6B; Rickart and Heaney, 2002).

COMPARISONS: Distinguished from *S. musseri,* n. sp., by the following features (tables 3, 4; figs. 9–11; Rickart et al., 1998: figs. 10, 12, 13; Balete et al., 2006: figs. 2–6): (1) larger body size overall; (2) relatively longer tail; (3) absolutely and relatively longer hind foot; (4) shorter and paler pelage; (5) flatter and lower cranium; (6) narrower interorbit; (7) narrower zygomatic breadth; (8) shorter nasals; (9) wider squamoso-mastoid vacuity; (10) shorter molar row; (11) narrower palate at M1; (12) narrower lingual palatal breadth at M3; (13) robust and broadly backswept coronoid process; (14) broader condyle; and (15) shorter, decurved angular process.

Distinguished from *S. montanus,* n. sp. (figs. 9, 14, 16; tables 3, 4), by the combination of the following features: (1) longer body size overall; (2) paler pelage; (3) relatively longer tail; (4) shorter skull with flatter cranium; (5) narrower interorbital region; (6) greater zygomatic breadth; (7) narrower mastoidal breadth; (8) shorter and shallower rostrum; (9) greater orbito-temporal length; (10) longer diastema; (11) longer postpalatal region; (12) wider incisors at their tips; (13) wider zygomatic plate.

Distinguished from *S. leonardocoi,* n. sp., by the following combination of features (figs. 9, 14, 17, tables 3, 4; Balete et al., 2006: figs. 2–6): (1) small body overall; (2) relatively longer tail; (3) relatively longer hind foot; (4) shorter, narrower skull; (5) lower and flatter braincase; (6) narrower interorbital region; (7) wider squamoso-mastoid vacuity; (8) longer diastema; (9) shorter postpalatal region; (10) shorter maxillary molar row; (11) smaller M1; (12) narrower palate at M1; (13) narrower labial breadth at M3; (14) broader incisors at their tips; (15) broader, more robust condyle; and (16) robust, backswept coronoid process.

A PCA analysis of cranial and dental measurements that included all species of *Archboldomys* and *Soricomys* (fig. 4, table 5) showed good separation from *S. leonardocoi,* n. sp., on the second axis, with *S. kalinga*, *S. montanus*, n. sp., and *S. musseri* having a proportionally longer skull, more elongate diastema and postpalatal region, and broader upper incisors near the tip, and *S. leonardocoi,* n. sp., having the converse. *Soricomys musseri*
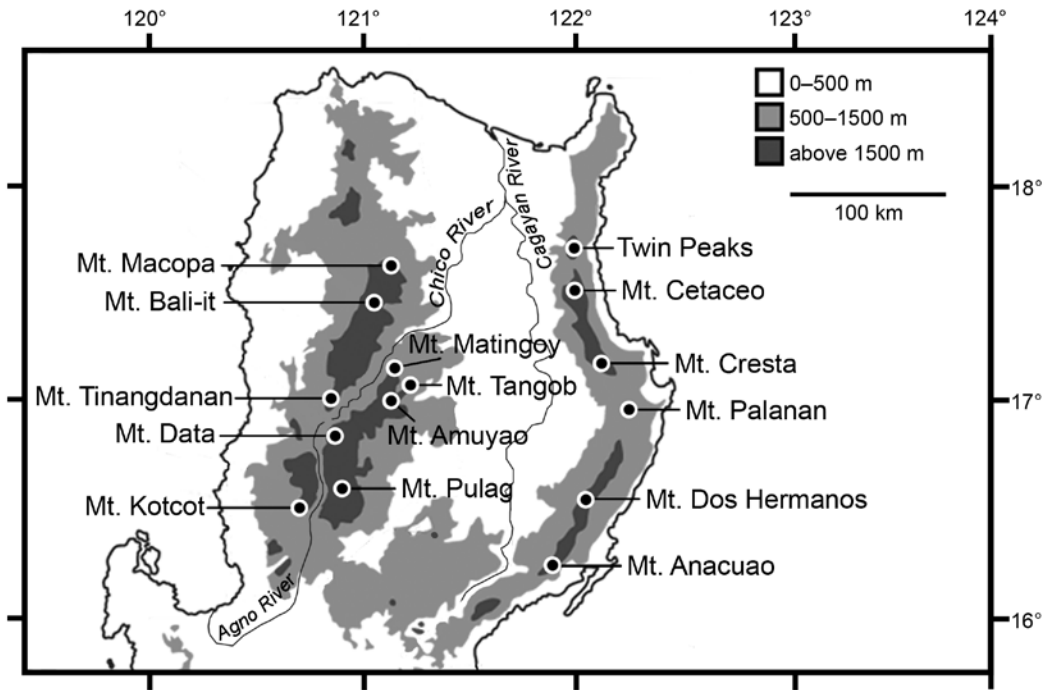
FIG. 15. Map of the Central Cordillera and Sierra Madre of northern Luzon, showing the locations of mountains and rivers discussed in the text.

differed from *S. kalinga* and *S. montanus* slightly on the first axis, an indication of its overall larger size. A second PCA that included only the four species of *Soricomys* (fig. 5, table 6) showed separation of *S. kalinga* from *S. musseri* and *S. leonardocoi*, n. sp., on the first component, primarily reflecting the overall larger size of those species. *Soricomys kalinga* overlapped with *S. montanus* extensively on the first two components, but had less overlap on the third and fourth components, indicating that *S. kalinga* tends to have greater zygomatic breadth, shorter incisive foramina, greater orbito-temporal fossa length, greater lingual breadth of palate at M3, and broader incisors near their tips, and greater post-postatal length and broader zygomatic plates.

DISTRIBUTION: *Soricomys kalinga* is currently known from the northern portion of the Central Cordillera of northern Luzon, where it has been documented at localities on Mt. Bali-it in Balbalan Municipality, Kalinga Province (figs. 1, 15). Inspection of figure 15 leads us to suggest that this species occurs north of the drainages of the Agno and Chico rivers (including the Sabangan river, a tributary of the Chico); these two drainages form a declivity across the crest of the Central Cordillera, with their headwaters meeting at a narrow pass that reaches a maximum elevation of about 1800 m, a short distance to the northwest of Mt. Data. On this basis, we hypothesize that this species will be found to occur from approximately Mt. Tinangdanan (ca. 5 km SW of Sagada) along the chain of mountains

stretching NNE to at least as far as Mt. Macopa, which lies along the boundary of Abra and Apayao provinces. The type locality lies slightly north of the center of this hypothesized distribution (fig. 15).

ECOLOGY: *Soricomys kalinga* occured in mature montane and mossy forest from ca. 1600 m to 2150 m on Mt. Bali-it in Balbalan Municipality, Kalinga Province, where it was predominantly diurnal and had significant preference for earthworm bait (Balete et al., 2006; Rickart et al., 2011a). The stomach contents included finely chewed arthropod exoskeletons, larval arthropods, and earthworms, suggesting an insectivore/vermivore feeding habit. Other species documented sympatrically with *S. kalinga* were: *Crocidura grayi*, *Apomys abrae*, *A. datae*, *A. microdon*, *A. musculus*, *Batomys granti*, *Bullimus luzonicus*, *Carpomys phaeurus*, *Chrotomys silaceus*, *Chrotomys whiteheadi*, *Rattus everetti*, and *Rhynchomys soricoides*; *Phloeomys pallidus* also occurred in the vicinity (Balete et al., 2006; Rickart et al., 2011a).

Females have two pairs of inguinal mammae. Males with scrotal testes were captured in February, and pregnancy was recorded in April: two pregnant females each bore two embryos, and one also had one placental scar (Balete et al., 2006).

COMMENTS: The karyotype (fig. 6B; initially reported as *A. musseri*; Rickart and Heaney, 2002) is based on a poor quality in vitro preparation. It is similar to *S. montanus,* n. sp. (2N = 44) and differs from *A. luzonensis* (2N = 26) as described above.

Soricomys montanus, new species
Figures 9, 12B, 14, 16

Archboldomys kalinga, Heaney et al., 2010 (part, included series from Mt. Amuyao, Mt. Data, and Mt. Pulag).

Archboldomys kalinga, Rickart et al., 2011a: 532 (part, included series from Mt. Amuyao, Mt. Data, and Mt. Pulag).

HOLOTYPE: FMNH 188314. Adult male collected on 3 March 2006; field number D.S. Balete 3788. Fresh tissues were removed from the thigh and placed in DMSO buffer. The rest of the specimen was initially fixed in formalin, now preserved in ethyl alcohol with skull removed and cleaned. It is currently housed at FMNH, but will be transferred to PNM.

TYPE LOCALITY: Philippines: Luzon Island: Mountain Province: 0.75 km N, 0.6 km E south peak of Mt. Data, 2241 m elevation, 16.86287° N, 120.86108° E (fig. 1).

MEASUREMENTS: Tables 3 and 4.

SPECIMENS EXAMINED (*N* = 18): Benguet Province, Bokod Municipality, Mt. Pulag National Park, 0.5 km S, 0.4 km W Mt. Babadak peak, 2480 m (FMNH 198175); Mountain Province: Barlig Municipality, Mt. Amuyao peak, 2690 m (FMNH 193516), 0.5 km N, 0.5 km W Mt. Amuyao peak, 2530 m (FMNH 193514, 193515), 0.75 km W Mt. Amuyao peak, 2300 m (FMNH 193517), 1.0 km N, 1.0 km W Mt. Amuyao peak, 2150 m (FMNH 193518–193520); Bauko Municipality, Mt. Data, 0.75 km E south peak, 2310 m (FMNH 188318), 0.75 km N, 0.6 km E south peak, 2241 m (FMNH 188314–188317), 0.75 km N, 0.75 km E south peak, 2289 m (FMNH 188319), 0.75 km N, 1.0 km E south peak, 2289 m (FMNH 188320, 188449).

ETYMOLOGY: From the Latin *montanus*, meaning "pertaining to mountains," in recognition of its distribution in the high mountains of the Central Cordillera, including Mountain Province. We suggest "southern Cordillera shrew mouse" as an English common name.

DIAGNOSIS: A slender-bodied member of *Soricomys*, distinguished from congeners by the following combination of features: (1) smaller body size overall; (2) shorter length of combined head and body; (3) pelage dark reddish brown dorsally, shorter and paler orange-brown ventrally; (4) greater rostral depth; (5) greater orbito-temporal length; (6) shorter postpalatal region.

DESCRIPTION AND COMPARISONS: *Soricomys montanus* is a small-bodied murid (20–31 g), with a tail equal to or slightly shorter than the combined length of head and body (table 3). The pelage of *S. montanus* is dark reddish brown dorsally, slightly shorter and paler ventrally (fig. 12B). The dorsal hair is tricolored, medium gray on the basal three-fourths, followed by a dark gray band with a reddish-brown distal quarter. The lips and rhinarium are pale grayish brown. The eyelids are edged in black, surrounded by a pale reddish-brown ring of short fur. The dark gray to black mystacial vibrissae are moderately long, extending beyond the ears. The ears are rounded, uniformly dark gray, and covered with short, dark

FIG. 16. Cranium and mandible of *Soricomys montanus*, adult male (FMNH 188314, holotype) in dorsal, ventral, and lateral views.

gray hairs. The hind feet are slender and with long digits bearing long, opaque claws. Their dorsal surface is uniformly grayish brown, darker on the plantar surface and plantar pads. The front feet of *S. montanus* are small and have slender digits bearing long, opaque claws with decurved tips, except the pollex, which is reduced to a stump and bears a nail. The dorsal surface of the forefeet and the palmar surface, including the palmar pads, is uniformly pale grayish brown.

Soricomys montanus is similar to congeners in overall body form, but closest to *S. kalinga* in most external features and body proportions (fig. 12B, table 3; Balete et al., 2006: fig. 3). It differs from the latter by the following combination of features: (1) smaller and shorter body overall (larger and longer in *S. kalinga*); (2) darker pelage (paler); and (3) shorter tail (longer). It is distinguished from *S. musseri* by the following combination of features: (1) smaller body overall;
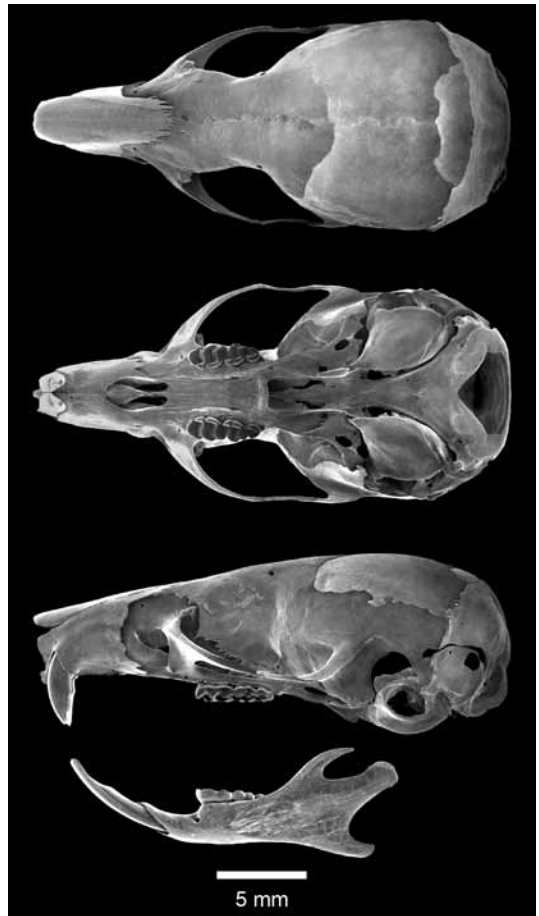
(larger); (2) longer tail (shorter); and (3) relatively longer hind foot (shorter), and from *S. leon-ardocoi,* n. sp., by the following traits: (1) shorter body overall (longer); (2) shorter, paler pelage (longer and darker); (3) relatively longer tail (shorter); and (4) relatively longer hind foot (shorter).

Soricomys montanus has a smooth skull, with a short and tapered rostrum (fig. 16). The cranium is longer than wide, appearing triangular in general outline. The lateral dorsal profile is nearly straight from the top of the skull to the tip of the rostrum. The nasals are straight, and extend to the level of the anterior edges of the premaxillae. The upper incisor root is enclosed in a barely raised bony capsule within the premaxilla and terminates close to the suture with the maxilla, fronting the dorsal opening of the narrow lachrymal canal. The zygomatic plate has a straight anterior edge, and is slightly arched dorsally. The zygomatic process of the squamosal is anchored about 1.5 mm above the dorsal edge of the postglenoid foramen. The tympanic hook of the squamosal is narrow and slender, with a caudad slant. The large mastoid fenestra is situated close to the posterior margin of the mastoid, opposite the elongate mastoid foramen that runs along the barely ossified occipital suture, and merging with the squamoso-mastoid foramen. Various stages of ossification of the occipital suture and separation of the mastoid and squamoso-mastoid foramina are evident among the paratypes.

The incisive foramina of *S. montanus* are small, round-edged posteriad and smoothly tapered anteriad; nearly half as long as the diastema (fig. 16, table 4). The alisphenoid canal is small and narrow, partly hidden under the pterygoid ridge (as seen from ventral view), but otherwise fully exposed in the holotype, due to the missing alisphenoid strut reminiscent of the *Crunomys* pattern, though only partially evident in *C. suncoides* (Musser, 1982a: fig. 23; Rickart et al., 1998: figs. 4, 7); in all the paratypes, however, the alisphenoid canal is positioned under the posterior edge of the thin pterygoid ridge, behind the short and narrow alisphenoid strut.

Because the pterygoid strut is absent in the holotype, the pterygoid ridge merges posteriad with the pterygoid bridge that extends over the foramen ovale to the anterior edge of the elongate middle lacerate foramen (fig. 16); in all the paratypes, as in the congeners, the pterygoid ridge terminates posteriad at its juncture with the alisphenoid strut (fig. 16; Rickart et al., 1998: fig. 12). The postglenoid vacuity is spacious and appears broadly triangular due to a blunt (and slightly arched) angle formed by the dorsal confluence of the backward-slanted anterior edge of the tympanic hook and forward-slanted posterior edge of the squamosal, with the straight ventral edge of the periotic part of the petromastoid as its base (fig. 16). This shape of the postglenoid vacuity in *S. montanus* approximates that of *S. kalinga*, but in the latter the shorter tympanic hook results in a pronounced anteriad skew (Balete et al., 2006: figs. 4–5); in contrast, it is smoothly arched in *S. musseri* (Rickart et al., 1998: figs. 6, 13; Balete et al., 2006: figs. 4–5) and somewhat rectangular in *S. leonardocoi,* n. sp. (fig. 17). The auditory bulla is relatively small and ventrolaterally inflated, gradually tapering anteriad and smoothly merging with the pointed eustachian tube (fig. 16); in all congeners, this anterior bullar inflation is conspicuous and forms a pronounced constriction that clearly demarcates the boundary with the narrow eustachian tube (figs. 10, 17; Rickart et al., 1998: figs. 12–13; Balete et al., 2006: fig. 4).

The skull of *S. montanus* closely resembles those of its congeners, but is most similar to *S. kalinga*. However, it can be distinguished from *S. kalinga* by the following combination of traits:

(1) longer skull with slightly dorsolaterally inflated cranium (shorter and dorsolaterally flattened in *S. kalinga*); (2) zygomatic breadth and zygomatic plate narrower (wider); (3) wider interorbit (narrower); (4) greater mastoidal breadth (narrower); and (5) longer, deeper rostrum (shorter and shallower). *Soricomys montanus* differs from *S. musseri* by the following combination of cranial features: (1) dorsolaterally flattened cranium (inflated in *S. musseri*); (2) narrower interorbit (broader); (3) zygomatic breadth narrower (broader); (4) broader zygomatic plate (narrower); (5) longer and deeper rostrum (shorter and shallower); (6) shorter nasals (longer); (7) shorter incisive foramina (longer); and (8) shorter orbito-temporal length (longer). *Soricomys montanus* can be distinguished from *S. leonardocoi,* n. sp., by the following combination of features: (1) shorter skull with dorsolaterally flattened cranium (longer and inflated in *S. leonardocoi,* n. sp.); (2) narrower interorbital region (wider); (3) greater zygomatic breadth (narrower); (4) narrrower zygomatic plate (wider); (5) longer and deeper rostrum (shorter and shallower); (6) shorter orbito-temporal length (longer); (7) longer diastema (shorter); and (8) shorter postpalatal region (longer).

The incisors of the new species are small and have smooth anterior surfaces, as is typical of all other species of *Soricomys*. The

FIG. 17. Cranium and mandible of *Soricomys leonardocoi*, adult male (FMNH 190972, holotype) in dorsal, ventral, and lateral views.

upper incisors have orange enamel and emerge from the rostrum at a right angle (orthodont). The lower incisors are long and thinly pointed and have paler enamel. The ventral tips of the upper incisors are nearly straight edged. In ventral view, the outline of the base of each forms a broad "U" shape canted laterally, so that the two incisors form a deep, V-shaped gap along their posteromedial margin (fig. 9). As with congeners, the upper molars are small and narrow. The first upper molar is roughly rectangular in outline, with the convex projection of cusps t1 and t4 forming a distinct bilobed and broadly tapered lingual outline. Cusp t3 is barely discernible in the shallow and sloping labial edge of the coalesced laminar outline of the first row of M1, and difficult to detect in specimens with heavily worn molars; t3 is undetectable in M2 and M3. In both M1 and M2, cusp t9 is barely detectable on the broad

laminar outline on their third row, which is largely comprised of the coalesced cusps t7 and t8. M3 is relatively large in relation to M1 and M2, with the broadly convex cusp t1 accounting for nearly half of its occlusal surface, and the rest formed by the coalesced cusps of the second row; the presence of the third row is not evident.

The dentition of *S. montanus* is similar to congeners, with differences evident mainly in relative sizes of teeth and cuspidation pattern (figs. 9, 14, 16, table 4; Balete et al., 2006: fig. 6; Rickart et al., 1998: fig. 8). The following combination of dental features readily distinguishes it from *S. kalinga* (figs. 10, 11): (1) slightly longer maxillary molar row (shorter in *S. kalinga*); (2) broader first upper molar, M1 (narrower); and (3) narrower incisors at their tips (broader). *Soricomys montanus* is distinguished from *S. musseri* by: (1) shorter maxillary molar tooth row (longer in *S. musseri*); (2) narrower M1 (broader); and (3) narrower incisors at tip (broader); and from *S. leonardocoi,* n. sp., by: (1) shorter maxillary molar tooth row (longer in *S. leonardocoi,* n. sp.); (2) narrower M1 (broader); and (3) wider incisors at their tips (narrower).

Soricomys montanus has mandibles that closely resemble those of its congeners in general shape and placement of mental and mandibular foramina. They differ mainly in relative size and shape of the processes (fig. 16, table 4; Balete et al., 2006: fig. 4; Rickart et al., 1998: fig. 13). The coronoid process is relatively long, robust, and broadly backswept to about two-thirds the length of the condyloid process. In contrast, the coronoid process of *S. kalinga* is shorter and slender, though equally broadly backswept; it is longer, more delicate, and narrowly backswept in *S. musseri*; in *S. leonardocoi,* n. sp., it is about as long but more slender. The condyloid process of *S. montanus* is more robust and its angular process relatively shorter than in congeners.

KARYOLOGY: 2N = 44; FN = 52 (fig. 6C).

DISTRIBUTION: Currently known from the southern portion of the Central Cordillera of northern Luzon, in Benguet Province and Mountain Province (fig. 1). As noted above, inspection of figure 15 leads us to suggest that this species occurs south of the drainages of the Agno and Chico rivers (including the Sabangan river, a tributary of the Chico). On this basis, we hypothesize that this species will be found from south of Mt. Pulag, possibly incuding the vicinity of Mt. Kotkot, near Baguio in Benguet Province, trending north and northeast past Mt. Pulag, Mt. Data, and Mt. Amuyao, ending near the level of Mts. Matingoy and Tangob, at the southern end of Kalinga Province at ca. 17°15′N, east of the Chico River. The type locality lies near the center of this distribution.

ECOLOGY: *Soricomys montanus* was recorded in old-growth and in lightly disturbed mossy forest from 1800 m to 2690 m on Mt. Amuyao; on Mt. Data it was recorded in heavily disturbed mossy forest at 2241–2310 m, and in similar forest on Mt. Pulag at 2480 m (Heaney et al., 2006, unpubl. specimens and field notes at FMNH; Rickart et al., 2011b). It showed a high level of tolerance to forest disturbance on Mts. Amuyao, Data, and Pulag, but was absent in heavily disturbed habitats dominated by pine forest or by agriculture at the elevations where they occurred (Rickart et al., 2011b). We found *S. montanus* to be predominantly diurnal and to show a preference for earthworm bait (Balete, Heaney, and Rickart field notes at FMNH). On Mt. Amuyao, five of six individuals examined for stomach contents had arthropod remains in their stomachs, and two of them had earthworms. A list of species that cooccurred with *S. montanus* on Mt. Amuyao is included in the species account for *Archboldomys maximus*, above.

Females have two pairs of inguinal mammae. On Mt. Amuyao, two of the four females caught in March had large mammae, but neither was pregnant; and four of the five males recorded during the same period had scrotal testes. On Mts. Data and Pulag, only males were documented and all had scrotal testes in March and April, respectively.

COMMENTS: Populations of *Soricomys montanus* from the three separate mountains (Amuyao, Data, and Pulag) exhibit little apparent variation in external, cranial, and dental features, suggesting their very close affinity (tables 3, 4). This species exhibits the highest intra-specific divergence values in cytochrome *b*, with populations from Mt. Amuyao differing from those from Mt. Data by 3% (fig. 7).

Soricomys leonardocoi, new species
Figures 9, 12C, 14, 17

HOLOTYPE: FMNH 190972. Adult male collected on 04 June 2006; field number D.S. Balete 4160. Fresh tissues removed from the thigh and placed in DMSO buffer. The rest of the speci-men was initially fixed in formalin, now preserved in ethyl alcohol with skull removed and cleaned. It is currently housed at FMNH, but will be transferred to PNM.

TYPE LOCALITY: Philippines: Luzon Island: Aurora Province: Dingalan Municipality: 0.9 km S, 0.3 km W Mt. Mingan peak, 1785 m elevation, 15.47390° N, 121.40066° E (fig. 1).

MEASUREMENTS: Tables 3 and 4.

SPECIMENS EXAMINED (N = 23): Aurora Province, Dingalan Municipality, Mt. Mingan, 0.9 km S, 0.3 km W Mt. Mingan peak, 1785 m elevation (FMNH 190970–190972 [holotype], 190973); 1.5 km S, 0.5 km W Mt. Mingan peak, 1681 m elevation (FMNH 190974–190979); 1.8 km S, 1.0 km W Mt. Mingan peak, 1677 m elevation (FMNH 190961–190969); 1.9 km S, 1.6 km W Mt. Mingan peak, 1476 m elevation (FMNH 190980–190982).

ETYMOLOGY: We name this species in honor of our colleague and friend Leonardo Co, who devoted his life to studying the plants of the Philippines and their medicinal uses, promoting conservation, improving the lives of his fellow Filipinos, and enhancing our knowledge of this unique and threatened flora.

DIAGNOSIS: A slender-bodied member of *Soricomys*, distinguished from congeners by the following combination of features: (1) larger body size; (2) longer, dark reddish-brown dorsal pelage, shorter and paler orange-brown ventrally; (3) relatively shorter tail; (4) wider interor-bital region; (5) wider zygomatic plate; (6) longer incisive foramina; (7) shorter diastema; (8) longer postpalatal region; (9) longer maxillary molar row; (10) broader first upper molars; and (11) narrower incisor breadth at their tips.

DESCRIPTION AND COMPARISONS: The pelage of *S. leonardocoi* is dark grayish chestnut dor-sally, pale grayish brown and shorter ventrally, without distinct patterning. The lips and rhinarium are medium gray (fig. 12C). Mystacial vibrissae are dark gray with pale tips that extend beyond the ears. The eyelids are dark gray surrounded by a narrow paler band covered with short, dark, grayish-brown fur. The dark gray ears are small, rounded, and covered with short, dark hairs. The front feet of *S. leonardocoi* are small, with long, slender digits bearing long, opaque claws with decurved tips, except the pollex, which is short and bears a nail. The dorsal surface is pigmented

medium grayish brown, and the palmar surface and palmar pads, consisting of three small inter-digitals and two larger pads (thenar and hypothenar), are paler and uniformly pigmented. The hind feet are long and slender, with long, slender digits bearing long, opaque claws. They are dorsally pigmented medium grayish brown, darker on the digits, and covered with grayish-brown fur; dark gray to pale grayish-brown ungual tufts extend to about three-quarters of the length of claws. The plantar surface is uniformly pigmented dark grayish brown; six plantar pads, consisting of four interdigitals, a thenar, and a hypothenar, are small relative to the plantar surface, and uni-formly pigmented the same darkness as the plantar surface except slightly paler at the distal tips.

Soricomys leonardocoi is similar to congeners in overall body form, but most similar to *S. musseri* in most external features and body proportions (fig. 12, table 3; Rickart et al., 1998: fig. 10). It is distinguished from the latter by the following external features: (1) longer and larger body (shorter in *S. musseri*); (2) absolutely and relatively longer hind foot with darkly pigmented plantar pads (absolutely and relatively shorter, with paler plantar pads); (3) longer, darker fur (shorter and pale yellowish brown); and (4) relatively shorter tail (longer). *Soricomys leonardocoi* is distinguished from *S. kalinga* by the following external characters (fig. 12C, table 3; Balete et al., 2006: fig. 3): (1) large body size overall (smaller in *S. kalinga*); (2) relatively shorter tail (longer); and (3) relatively shorter hind foot (longer); and from *S. montanus* by: (1) longer body overall (shorter in *S. montanus*); (2) longer, darker pelage (shorter and paler); (3) relatively shorter tail (longer); and (4) relatively shorter hind foot (longer).

The skull of *S. leonardocoi*, as in congeners, is smooth and the braincase is longer than wide, appearing rectangular in general outline. The rostrum is short and tapered. Laterally, the dorsal profile is nearly straight from the top of the skull to the tip of the rostrum. The nasals of *S. leon-ardocoi* are straight, and terminate near the level of the anterior edges of the premaxillae. The upper incisor root is enclosed in a slightly raised bony capsule within the premaxilla and termi-nates medially near the suture with the maxilla, opposite the dorsal opening of the small and narrow lachrymal canal. The opening of this canal slants caudad and its swollen outer wall con-spicuously broadens the base of the rostrum. The zygomatic plate has a nearly straight, vertical anterior edge relative to the upper molar row. The zygomatic process of the squamosal is anchored posteriorly about 1 mm above the dorsal edge of the postglenoid foramen and attached higher laterally on the cranium. The tympanic hook of the squamosal is broadly tapered ventrad and slanted caudad. This broadening of the tympanic hook dorsally is coupled by the intrusion mediolaterally of a small bony mastoidal spur into the squamoso-mastoid foramen, resulting in a very narrow opening (fig. 17). A relatively large mastoid fenestra is near the posterior margin of the mastoid, opposite the small mastoid foramen along the occipital suture (fig. 17).

In ventral aspect of the skull, the incisive foramina of *S. leonardocoi* are small, round edged posteriad and smoothly tapered anteriad; they are slightly more than half the length of the diastema (fig. 17, table 4). The alisphenoid canal is small and narrow. It is positioned under the posterior edge of the thin pterygoid ridge, behind the short and narrow alisphenoid strut. The pterygoid ridge itself terminates posteriad at the juncture with the alisphenoid strut, opposite which a relatively wide pterygoid bridge extends over the foramen ovale to the anterior edge of the elongate middle lacerate foramen. The postglenoid vacuity is relatively spacious and appears rectangular due to its straight

dorsal edge (domed in congeners), and an almost straight ventral edge formed by the periotic part of the petromastoid (fig. 17). The auditory bulla is relatively small and ventrolaterally inflated, obscuring as much as the anterior half of the petrosal in ventral view. *Soricomys kalinga* and *S. montanus* have a similar pattern of bullar inflation; it is less pronounced in *S. musseri*.

The cranial features of *S. leonardocoi* are similar to all congeners, but most similar to *S. musseri* (figs. 10, 11, table 4; Balete et al., 2006: figs. 4, 5; Rickart et al., 1998: figs. 8–10, 13, 14). However, subtle but consistent differences are evident between *S. leonardocoi* and *S. musseri*, and the following combination of features distinguishes the former from the latter: (1) slightly longer skull (shorter in *S. musseri*); (2) shorter nasals (longer); (3) longer incisive foramina (shorter); (4) narrower interorbital region (broader); (5) narrower zygomatic breadth (broader); (6) broader zygomatic plate with nearly straight anterior edge (narrower with slightly concave anterior edge); (7) long and slender squamosal strut (shorter and broader); (8) larger squamoso-mastoid vacuity; (9) narrower alisphenoid strut (wider), and (10) narrower pterygoid bridge (wider). *Soricomys leonardocoi* is distinguished from *S. kalinga* by the following combination of cranial features (figs. 9–11, 14, 17, table 4; Balete et al., 2006: figs. 4, 5): (1) longer and larger skull (shorter, narrower skull in *S. kalinga*); (2) dorsolaterally inflated cranium (lower and flatter braincase; (3) broader interorbit (narrower); 4) narrower squamoso-mastoid vacuity (larger); (5) shorter diastema (longer); and (6) longer postpalatal region (shorter); and from *S. montanus* by: (1) longer skull with inflated cranium (shorter and flatter in *S. montanus*); (2) wider interorbital region (narrower); (3) narrower zygomatic breadth (wider); (4) wider zygomatic plate (narrower); (5) shorter and shallower rostrum (longer and deeper); (6) shorter diastema (longer); and (7) greater orbito-temporal length (shorter).

The incisors of *Soricomys leonardocoi* are small and have smooth anterior surfaces. The upper incisors emerge from the rostrum at a right angle (orthodont) and have yellowish-orange enamel. The ventral tips are nearly straight edged. In ventral view, the outline of each incisor is U-shaped deflected laterally, forming a deep, V-shaped gap along their posteromedial margin (fig. 9). The lower incisors are long and thinly pointed and have pale yellow enamel. The upper molars are small and narrow, but with low and sloping labial cusps that do not have corresponding convexity. The first upper molar is only slightly more than half as wide as it is long, and appears roughly rectangular in outline (especially in individuals with worn molars). The convex projection of cusps t1 and t4 forms a distinct, shallowly bilobed and broadly tapered lingual outline on M1. Cusp t3 appears to be present in the shallow and sloping labial edge of the coalesced laminar outline of the first row of M1, but is difficult to detect in most specimens with worn molars; t3 is undetectable on M2. Cusp t9 in both M1 and M2 is barely detectable on the broad laminar outline on the third row. M3 is relatively large in relation to M1 and M2, with the broadly convex cusp t1 accounting for about a third of the occlusal surface of this molar.

The dentition of *S. leonardocoi* is closely similar to congeners, differing mainly in relative sizes and cuspidation pattern (figs. 9, 14, 17, table 4; Balete et al., 2006: fig. 6; Rickart et al., 1998: fig. 8). It is readily distinguishable from *S. musseri* by the following combination of dental features: (1) longer maxillary molar tooth row (shorter in *S. musseri*); (2) broader M1 (narrower); and (3) narrower incisors at their tips (broader), and from *S. kalinga* and *S. montanus*

by: (1) longer maxillary molar tooth row (shorter in *S. kalinga* and *S. musseri*); (2) broader first upper molar, M1 (smaller); (3) greater palatal breadth at M1 (narrower); (4) greater labial breadth at M3 (narrower); and (5) narrower incisors at their tips (broader).

The mandible of *S. leonardocoi* is closely similar to congeners in general shape and placement of mental and mandibular foramina, differing mainly in relative size and shape of the processes (fig. 17, table 4; Balete et al., 2006: fig. 4; Rickart et al., 1998: fig. 13). The coronoid process is relatively short and broadly slanting to about two-thirds the length of the slender condyloid process. In contrast, the coronoid process of *S. kalinga* is about as long, but more robust than in the new species; it is more delicate in *S. musseri* (fig. 10). The angular process of *S. leonardocoi* is slender and narrowly tapered; it is robust and broadly tapered in *S. kalinga* and *S. montanus*; slender, broadly angled and nearly straight edged dorsally in *S. musseri*.

Distribution: Currently known only from the Mingan Mountains, in the Central Sierra Madre (fig. 1).

Ecology: We found *Soricomys leonardocoi* in montane and mossy forest from 1476 m to 1785 m elevation (Balete et al., 2011). It appeared to be active both day and night, with almost equal numbers of diurnal and nocturnal/crepuscular captures (Balete et al., 2011). In contrast, *S. kalinga*, *S. montanus*, and *S. musseri* appeared to be predominantly diurnal (Balete et al., 2006, 2011; Duya et al., 2011; Rickart et al., 2011a; Balete and Heaney, unpubl. data). Individuals were significantly more frequently caught with earthworm bait than coconut bait, indicating vermivorous habits (Balete et al., 2011). *Soricomys kalinga* had similar statistically significant response to earthworm bait; *S. musseri* also was similar, but the sample size was small (Balete et al., 2006; Duya et al., 2011; Rickart et al., 2011a). Females have two pairs of inguinal mammae, as do congeners. Four of nine females caught in June had large mammae, but none was pregnant or lactating. A single male caught in late May had scrotal testes, as did six of seven during June.

We documented six members of the *Chrotomys* Division to occur sympatrically with *S. leonardocoi* on Mt. Mingan: *Apomys microdon*, *A. musculus*, *A. aurorae*, *A. minganensis*, and *Rhynchomys* sp.; another member of this clade, *Chrotomys* cf. *mindorensis*, occurred at ca. 100 m, in a reforestation site planted with exotic species of trees (table 11; Balete et al., 2011; Heaney et al., 2011). *Crocidura grayi*, *Bullimus luzonicus*, *Phloeomys pallidus*, and *Rattus everetti* also occurred sympatrically with *S. leonardocoi* on Mt. Mingan (Balete et al., 2011).

DISCUSSION

As forewarned by Musser (1982b: 2), "the diversity of the fauna [of the Philippines], at the level of genera and species, is greater than generally realized." The descriptions of a new genus and species (*Musseromys gulantang*; Heaney et al., 2009), a new subgenus and seven new species of *Apomys* (Heaney et al., 2011), two new species of *Rhynchomys* (Balete et al., 2007), one new species of *Chrotomys* (Rickart et al., 2005), one new species of *Limnomys* (Rickart et al., 2003), one new species of *Bullimus* (Rickart et al., 2002), and the new genus and three new species described here make it clear that the murid rodents, in particular, are much more diverse than had been recognized even within the last decade. This diversity has been detected

through targeted surveys of isolated mountains and mountain chains, using multiple sampling procedures to ensure detection of species that have varied food and foraging habits in different habitats along the elevational gradient (e.g., Balete et al., 2009; Heaney et al., 2011; Rickart et al., 2011a, 2011b). In the case of *Archboldomys* and *Soricomys*, the use of live earthworms as bait, the targeting of montane and mossy forest at high elevations, and surveys of even small mountain chains, have been crucial in detecting the animals.

<div align="center">Phylogenentic Relationships</div>

Our analyses of DNA sequence data from the mitochondrial cytochrome *b* (fig. 7) and the nuclear IRBP (fig. 8) genes provide robust evidence that the *Chrotomys* Division is a monophyletic unit, as first documented by Jansa et al. (2006). As discussed above, our earlier studies of morphology led us to view *Archboldomys* as a monophyletic unit containing two "species groups," but the genetic data presented here provide unambiguous evidence that these two "species groups" are not sister taxa, but rather are distantly related members of the *Chrotomys* Division. Many of the morphological similarities that we previously interpreted as homologies (e.g., dark reddish-brown pelage both dorsally and ventrally, tail of moderate length, reduced dentition) may represent convergent characters, perhaps associated with the largely diurnal habit of foraging for earthworms, insects, and other invertebrates in leaf litter. The extent of ecological differences that allow syntopy of *A. maximus* with *S. kalinga* on Mt. Amuyao (and possibly more widely within the Central Cordillera) may now be seen as especially important in understanding the evolution of diversity within the *Chrotomys* Division, and deserve further investigation. Moreover, the sister-group relationship of *Soricomys* with *Chrotomys* now becomes one of special interest, with the implication that the burrowing habit of *Chrotomys* is a feature derived since divergence from the ancestor shared with the more generalized *Soricomys*. Detailed studies of the anatomy and character evolution in the *Chrotomys* Division, including changes in limbs and feet, might provide insights on the factors facilitating coexistence.

The karyotype of *Soricomys montanus* is very similar to those of several members of the *Chrotomys* Division, including species in the genera *Chrotomys, Rhynchomys,* and the *Apomys* subgenus *Megapomys* that have karyotypes with 2N = 44 and FN = 52 to 58 with a majority of telocentric chromosomes (table 7; Rickart and Musser, 1993; Rickart and Heaney, 2002; Heaney et al., 2011). The 2N = 44 karyotype of *S. kalinga*, while imperfectly known, also is consistent with this group. The occurrence of this widespread 2N = 44 karyotype in taxa positioned throughout the clade strongly suggests that it represents a primitive arrangement for the Chrotomys Division. In contrast, the karyotype of *Archboldomys luzonensis* is unique among Philippine murids examined to date, both in basic arrangement of the autosomes and in the apparently unique sex chromosome system (Rickart and Musser, 1993). The position of *A. luzonensis* within the *Chrotomys* Division (fig. 7; see also Jansa et al., 2006: fig. 1) indicates that this karyotype is a distinctive, highly derived condition. Unfortunately, the karyotypes of *A. maximus, S. leonardocoi*, and *S. musseri* are unknown, so that the utility of the unique features of the *A. luzonensis* karyotype in defining and contrasting the two genera remain unknown.

BIOGEOGRAPHY

Members of the *Chrotomys* Division are endemic to the Philippine Islands, with greatest diversity on Luzon. All species of *Archboldomys*, *Rhynchomys*, and *Soricomys* are restricted to Luzon. *Chrotomys* is represented by at least four species on Luzon, and by single species on Mindoro and Sibuyan. The many species of *Apomys* occur widely in the Philippines with the exceptions of the Batanes and Babuyan island groups (north of Luzon), the Palawan region, and the Sulu Archipelago (between Mindanao and Borneo; Balete et al., 2007; Heaney, 1986; Heaney et al., 1998; Rickart et al., 2005; Steppan et al., 2003). Within Luzon, several clear patterns of distribution are evident.

(1) The number of species of nonvolant small mammals, including members of the *Chrotomys* Division, increases with increasing elevation up to about 2200 m, with a slight decline in species richness above that level (Heaney, 2001; Rickart et al., 2011a).

(2) The total number of species of nonvolant small mammals on any given mountain is positively correlated with the height of the mountain on which they occur; because the Central Cordillera has the highest mountains, it has the largest number of species. These patterns hold for the *Chrotomys* Division (table 12), as well as more broadly (Heaney and Rickart, 1990; Heaney, 2001; Rickart et al., 2011a).

(3) On the lower (and therefore more species-poor) mountains, there are typically two species of *Apomys*, one *Chrotomys*, and one *Archboldomys* or *Soricomys*. On the highest (and most species-rich) mountains, there are up to four species of *Apomys*, one *Archboldomys*, two *Chrotomys*, one *Rhynchomys*, and one *Soricomys* (table 12).

(4) With up to nine species documented on a single mountain (Mt. Amuyao), members of the *Chrotomys* Division—an endemic, monophyletic group—are the most speciose and abundant component of the small mammal community (e.g., Rickart et al., 1991, 2011a, 2011b; Balete et al., 2009; Heaney et al., 2011).

(5) Each species of *Archboldomys* and *Soricomys* occurs only in montane and mossy forest habitats from ca. 1350–2690 m.

(6) Each species of *Archboldomys* and *Soricomys* is confined to an isolated mountain (e.g., Mt. Cetaceo, Mt. Isarog, Mt. Mingan) or chain of mountains in an isolated mountain range (e.g., mounts Amuyao, Data, and Pulag in the southern Central Cordillera), each of which is a center of endemism with several endemic mammals (fig. 1; Balete et al., 2006, 2007, 2011; Duya et al., 2011; Heaney et al., 1999, 2005, 2011; Rickart et al., 1991, 2011a, 2011b). The presence of two species of *Soricomys* (*S. kalinga* and *S. montanus*) in the northern and southern Central Cordillera, respectively, reflects the least geographic isolation, separated respectively to the north and south of the cleft in the Central Cordillera created by the Chico-Sabangan drainage (which runs north) and the Agno River (which runs south), which meet at a narrow pass that reaches ca. 1800 m (fig. 15). With the exception of the division between northern and southern Central Cordillera, the other members of the *Chrotomys* Division (*Apomys*, *Chrotomys*, and *Rhynchomys*) exhibit the same pattern of distribution, and further illustrate how isolation of mountain habitats provides another level of insularization that contribute to the observed richness of mammalian diversity in this isolated oceanic island (Balete et al., 2006, 2007; Heaney, 2000; Heaney et al., 2011; Rickart et al., 1998, 2005; Musser and Freeman, 1981; Steppan et al., 2003).

(7) The community composition of the nonvolant small mammals on each mountain or mountain range further illustrates the breadth and range of adaptive radiation in the *Chrotomys* Division (table 12; Balete et al., 2006, 2007, 2011; Duya et al., 2011; Heaney et al., 1999, 2005; Jansa et al., 2006; Rickart et al., 1991, 2011a). We have recorded six members of this clade occurring at a single locality on Mt. Bali-it (Rickart et al., 2011a), and seven at a locality on Mt. Amuyao (Rickart et al., 2011b; Heaney et al., unpubl. data and specimens at FMNH). We currently have evidence of species of *Archboldomys* and *Soricomys* occurring sympatrically only in the Central Cordillera, on Mt. Amuyao, where both species were predominantly diurnal, were captured in leaf litter on the ground surface, showed preference for earthworm bait, and had remains of invertebrates in their stomachs (see species accounts above). We note that adult *A. maximus* average about 45 g and *S. montanus* about 27 g, which may indicate some difference in trophic level or foraging activities. Clearly, communities of murid rodents on Luzon are often comprised of many closely related species. All members of the *Chrotomys* Division are thought to be descended from a species that reached the Philippines ca. 12–15 Mya (Jansa et al., 2006).

Conservation

Soricomys montanus is widespread in the southern portion of the Central Cordillera, where it maintains populations in both old-growth and secondary forest, and even occurs in small patches of highly degraded forest on Mt. Data (Rickart et al., 2011b). *Archboldomys maximus* and *S. leonardocoi* are members of a rich assemblage of endemic mammals associated with montane and mossy forest on Mt. Amuyao and Mt. Mingan, respectively. These new species appeared to be in moderate but stable populations in their respective habitats, as with the other members of the small mammal community there. Their habitats have not been subjected to the extensive logging that has drastically reduced the lowland dipterocarp forest of much of Luzon and the rest of the Philippines (Environmental Studies for Social Change, 1999). On both Mt. Amuyao and Mt. Mingan, high-elevation habitats are still in good condition. However, we noted that on Mt. Amuyao, construction of telecommunication facilities on the peak, with accompanying forest clearing along the route from the town center to the peak, have increased forest loss in the area. Additional negative impacts, including recent forest fires from the increasing number of mountain climbers and hikers, were also evident along the trails. Mt. Mingan, on the other hand, had much lesser signs of disturbance away from populated areas.

On both mountains, and over large portions of the Central Cordillera, the indigenous tribes continue to manage the forests following their traditional customs and are responsible for keeping the forest largely protected. Mt. Bali-it and the adjacent mountains in Kalinga are managed through traditional practices by the Banao tribe (Heaney et al., 2005). In contrast, for instance, Mt. Data National Park, which is managed by the national government, has lost much of the high elevation forest to commercial vegetable farming (Heaney et al., 2006). During our fieldwork there in 2006 we documented *S. montanus* along the grassy edge of a trail within the remnant mossy forest. However, we failed to find *Chrotomys silaceus* and *Rhynchomys soricoides*, first discovered there by John Whitehead in 1895, or *Abditomys latidens,* found on Mt. Data in 1946 (Musser, 1982b; Thomas, 1895, 1898; Sanborn, 1952). At least four more species docu-

mented on Mt. Data appeared to have become locally extinct by 1946: *Carpomys melanurus*, *C. phaeurus*, *Crateromys schadenbergi*, and *Phloeomys pallidus* (Thomas, 1898; Sanborn, 1952). Mt. Pulag, like Mt. Data, is currently undergoing extensive deforestation associated with commercial vegetable farming (table 12; Rickart et al., 2011b).

The beneficial effects of traditional management of the forest resources by the indigenous peoples are an important factor in the conservation of the forest and its rich biodiversity in Balbalasang, Kalinga Province (Heaney et al., 2005). We caution against the marginalization of sustainable traditional practices of the indigenous peoples in the process of formalizing and centralizing management decisions in protected areas, as demonstrated on Mt. Data, which, ironically, is a national park. Management interventions aimed at encouraging and further strengthening the traditional forest resource use practices by indigenous peoples on Mt. Amuyao and Mt. Mingan may be an important contribution to the conservation of the unique mammalian diversity in these areas, as an integral part of the creation and/or management of protected areas to ensure the long-term sustainability of biodiversity protection and conservation of these mountains (Balete et al., 2011; Heaney et al., 2011; Rickart et al., 2011b).

ACKNOWLEDGMENTS

REFERENCES

Aplin, K.P., and K.M. Helgen. 2010. Quaternary murid rodents of Timor. Part I: new material of *Coryphomys buehleri* Schaub, 1937, and description of a second species of the genus. Bulletin of the American Museum of Natural History 341: 1–80.

Balete, D.S., and L.R. Heaney. 1997. Density, biomass, and movement estimates for murid rodents in mossy forest on Mt. Isarog, southern Luzon, Philippines. Ecotropica 3: 91–100.

Balete, D.S., E.A. Rickart, and L.R. Heaney. 2006. A new species of the shrew mouse, *Archboldomys* (Rodentia: Muridae: Murinae), from the Philippines. Biodiversity and Systematics 4: 489–501.

Balete, D.S., E.A. Rickart, R.G.B. Rosell-Ambal, S. Jansa, and L.R. Heaney. 2007. Description of two new species of *Rhynchomys* Thomas (Rodentia: Muridae: Murinae) from Luzon Island, Philippines. Journal of Mammalogy 88: 287–301.

Balete, D.S., L.R. Heaney, M.J. Veluz, and E.A. Rickart. 2009. Diversity patterns of small mammals in the Zambales Mts., Luzon, Philippines. Mammalian Biology 74: 456–466.

Balete, D.S. et. al. 2011. The mammals of the Mingan Mountains, Luzon: evidence for a new center of mammalian endemism. Fieldiana: Life and Earth Sciences 2: 75–87.

Brown, J.C. 1971. The description of mammals 1. The external characters of the head. Mammal Review 1: 151–168.

Brown, J.C., and D.W. Yalden. 1973. The description of mammals 2. Limbs and locomotion of terrestrial mammals. Mammal Review 3: 107–134.

Danielsen, F. et. al. 1994. Conservation of biological diversity in the Sierra Madre Mountains of Isabela and southern Cagayan Province, the Philippines. Manila: DENR–Birdlife International. 146 pp.

Drummond, A.J. et. al. 2006. Geneious v2.5.4, Internet resource (http://www.geneious.com/).

Duya, M.R.M., P.A. Alviola, M.V. Duya, D.S. Balete, and L.R. Heaney. 2007. Report on a survey of mammals of the Sierra Madre Range, Luzon Island, Philippines. Banwa 4: 41–68.

Duya, M.R.M, M.V. Duya, P.A. Alviola, D.S. Balete, and L.R. Heaney. 2011. Diversity of small mammals in montane and mossy forests on Mount Cetaceo, Cagayan Province, Luzon. Fieldiana: Life and Earth Sciences 2: 88–95.

Edgar, R.C. 2004. MUSCLE: multiple sequence alignment with high accuracy and high throughput. Nucleic Acids Research 32: 1792–1797.

Ellerman, J.R. 1941. The families and genera of living rodents. Vol. 2, Muridae. London: British Museum (Natural History).

Environmental Science for Social Change. 1999. Decline of the Philippine forest. Makati City: Bookmark Inc.

Esselstyn, J.A., R.M. Timm, and R.M. Brown. 2009. Do geological or climatic processes drive speciation in dynamic archipelagos? The tempo and mode of diversification in Southeast Asian shrews. Evolution 63: 2595–2610.

Esselstyn, J.A., S.P. Maher, and R.M. Brown. 2011. Species interactions during diversification and community assembly in an island radiation of shrews. PLoS ONE 6 (7): 1–13.

Heaney, L.R. 1986. Biogeography of mammals in Southeast Asia: estimates of rates of colonization, extinction, and speciation. Biological Journal of the Linnean Society 28: 127–165.

Heaney, L.R. 2000. Dynamic disequilibrium: a long-term, large-scale perspective on the equilibrium model of island biogeography. Global Ecology and Biogeography 9: 59–74.

Heaney, L.R. 2001. Small mammal diversity along elevational gradients in the Philippines: an assessment of patterns and hypotheses. Global Ecology and Biogeography 10: 15–39.

Heaney, L.R., and E.A. Rickart. 1990. Correlations of clades and clines: geographic, elevational, and phylogenetic distribution patterns among Philippine mammals. In G. Peters and R. Hutterer (editors), Vertebrates in the tropics: 321–332. Bonn: Museum Alexander Koenig.

Heaney, L.R., P.D. Heideman, E.A. Rickart, R.C.B. Utzurrum, and J.S.H. Klompen. 1989. Elevational zonation of mammals in the central Philippines. Journal of Tropical Ecology 5: 259–280.

Heaney, L.R. et. al. 1998. A synopsis of the mammalian fauna of the Philippine Islands. Fieldiana Zoology (new ser.) 88: 1–61.

Heaney, L.R., D.S. Balete, E.A. Rickart, R.C.B. Utzurrum, and P.C. Gonzales. 1999. Mammalian diversity on Mt. Isarog, a threatened center of endemism on southern Luzon Island, Philippines. Fieldiana Zoology (new ser.) 95: 1–62.

Heaney, L.R. et. al. 2005. Preliminary report on the mammals of Balbalasang, Kalinga Province, Luzon. Sylvatrop 13: 59–72.

Heaney, L.R., D.S. Balete, J. Sarmiento, and P. Alviola. 2006. Losing diversity and courting disaster: the mammals of Mt. Data National Park. Haring Ibon 25: 15–23.

Heaney, L.R., D.S. Balete, E.A. Rickart, M.J. Veluz, and S.A. Jansa. 2009. A new genus and species of small 'tree-mouse' (Rodentia, Muridae) related to the Philippine giant cloud rats. Bulletin of the American Museum of Natural History 331: 205–229.

Heaney, L.R. et. al. 2010. Synopsis of Philippine mammals. Field Museum of Natural History. Internet resource (http://www.fieldmuseum.org/philippine_mammals/).

Heaney, L.R. et. al. 2011. Seven new species and a new subgenus of forest mice (Rodentia: Muridae: Apomys) from Luzon Island. Fieldiana: Life and Earth Sciences 2: 1–60.

Jansa, S.A., and M. Weksler. 2004. Phylogeny of muroid rodents: relationships within and among major lineages as determined by IRBP gene sequences. Molecular Phylogenetics and Evolution 31: 256–276.

Jansa, S.A., F.K. Barker, and L.R. Heaney. 2006. The pattern and timing of diversification of Philippine endemic rodents: evidence from mitochondrial and nuclear gene sequences. Systematic Biology 55: 73–88.

Jansa, S.A., T.C. Giarla, and B.J. Lim. 2009. The phylogenetic position of the rodent genus *Typhlomys* and the global origin of Muroidea. Journal of Mammalogy 90: 1083–1094.

McGuire, J.A., C.C. Witt, D.L. Altshuler, J.V. Remsen. 2007. Phylogenetic systematics and biogeography of hummingbirds: Bayesian and maximum likelihood analyses of partitioned data and selection of an appropriate partitioning strategy. Systematic Biology 56: 837–856.

Misonne, X. 1969. African and Indo-Australian Muridae. Evolutionary trends. Musée royal de l'Afrique centrale (Tervuren) 172: 1–219.

Musser, G.G. 1982a. Results of the Archbold Expeditions. No. 110. *Crunomys* and the small-bodied shrew rats native to the Philippines and Sulawesi (Celebes). Bulletin of the American Museum of Natural History 174: 1–95.

Musser, G.G. 1982b. Results of the Archbold Expedition. No. 107. A new genus of arboreal rat from Luzon Island in the Philippines. American Museum Novitates 2730: 1–23.

Musser, G.G., and M.D. Carleton. 2005. Superfamily Muroidea. *In* D.E. Wilson and D.M Reeder (Editors), Mammal species of the world, a taxonomic and geographic reference: 894–1531. Baltimore, MD: Johns Hopkins University Press.

Musser, G.G., and P.W. Freeman. 1981. A new species of *Rhynchomys* (Muridae) from the Philippines. Journal of Mammalogy 62: 154–159.

Musser, G.G., and L.R. Heaney. 1992. Philippine rodents: definitions of *Tarsomys* and *Limnomys* plus a preliminary assessment of phylogenetic patterns among native Philippine murines (Murinae, Muridae). Bulletin of the American Museum of Natural History 211: 1–138.

Nylander, J.A.A. 2004. MrModeltest v2. Program distributed by the author. Evolutionary Biology Centre, Uppsala University.

Olson, L.E., and S.M. Goodman. 2003. Phylogeny of Madagascar's tenrecs (Lipotyphla, Tenrecidae). *In* S.M. Goodman and J.P. Benstead (editors), Natural history of Madagascar: 1235–1242. Chicago: University of Chicago Press.

Patton, J.L. 1967. Chromosome studies of certain pocket mice, genus *Perognathus* (Rodentia: Heteromyidae). Journal of Mammalogy 48: 27–37.

Rambaut, A., and A.J. Drummond. 2007. Tracer v1.4, Internet resource (http://beast.bio.ed.ac.uk/Tracer).

Rickart, E.A., and L.R. Heaney. 2002. Further studies on the chromosomes of Philippine rodents (Muridae: Murinae). Proceedings of the Biological Society of Washington 115: 473–487.

Rickart, E.A., and G.G. Musser. 1993. Philippine rodents: chromosomal characteristics and their significance for phylogenetic inference among 13 species (Rodentia: Muridae: Murinae). American Museum Novitates 3064: 1–34.

Rickart, E.A., L.R. Heaney, and M.J. Rosenfeld. 1989. Chromosomes of ten species of Philippine fruit bats (Chiroptera: Pteropodidae). Proceedings of the Biological Society of Washington 102: 520–531.

Rickart, E.A., L.R. Heaney, and R.C.B. Utzurrum. 1991. Distribution and ecology of small mammals along an elevational transect in southeastern Luzon, Philippines. Journal of Mammalogy 72: 458–469.

Rickart, E.A., L.R. Heaney, B.R. Tabaranza, Jr., and D.S. Balete. 1998. A review of the genera *Crunomys* and *Archboldomys* (Rodentia: Muridae: Murinae), with descriptions of two new species from the Philippines. Fieldiana Zoology (new ser.) 89: 1–24.

Rickart, E.A., L.R. Heaney, and B.R. Tabaranza, Jr. 2002. Review of *Bullimus* (Muridae: Murinae) and description of a new species from Camiguin Island, Phillipines. Journal of Mammalogy 83: 421–436.

Rickart, E.A., L.R. Heaney, and B.R. Tabaranza Jr. 2003. A new species of *Limnomys* (Rodentia: Muridae: Murinae) from Mindanao Island, Philippines. Journal of Mammalogy 84: 1443–1455.

Rickart, E.A., L.R. Heaney, S.M. Goodman, and S. Jansa. 2005. Review of the Philippine genera *Chrotomys* and *Celaenomys* (Murinae) and description of a new species. Journal of Mammalogy 86: 415–428.

Rickart, E.A., L.R. Heaney, D.S. Balete, and B.R. Tabaranza Jr. 2011a. Small mammal diversity along an elevational gradient in northern Luzon, Philippines. Mammalian Biology 76: 12–21.

Rickart, E.A., D.S. Balete, R.J. Rowe, and L.R. Heaney. 2011b. Mammals of the northern Philippines: tolerance for habitat disturbance and resistance to invasive species in an endemic insular fauna. Diversity and Distributions 17: 530–541.

Ronquist, F., and J.P. Huelsenbeck. 2003. MRBAYES 3: Bayesian phylogenetic inference under mixed models. Bioinformatics 19: 1572–1574.

Rowe, K.C., M.L. Reno, D.M. Richmond, R.M. Adkins, and S.J. Steppan. 2008. Pliocene colonization and adaptive radiations in Australia and New Guinea (Sahul): multilocus systematics of the old endemic rodents (Muroidea: Muridae). Molecular Phylogenetics and Evolution 47: 84–101.

Sanborn, C.C. 1952. Philippine zoological expedition 1946–1947. Mammals. Fieldiana: Zoology 33: 89–158.

Simpson, G.G. 1945. The principles of classification and a classification of mammals. Bulletin of the American Museum of Natural History 85: 1–350.

SPSS, Inc. 2000. SYSTAT 10. Chicago, IL: SPSS, Inc.

Steppan, S.J., C. Zawadzki, and L.R. Heaney. 2003. Molecular phylogeny of the endemic Philippine rodent *Apomys* (Muridae) and the dynamics of diversification in an oceanic archipelago. Biological Journal of the Linnean Society 88: 699–715.

Swofford, D. 2002. PAUP*: Phylogenetic analysis using parsimony (and other methods), 4.0 beta version for UNIX. Sunderland, MA: Sinauer Associates.

Thomas, O. 1895. Preliminary diagnoses of new mammals from northern Luzon, collected by Mr. John Whitehead. Annals and Magazine of Natural History (series 6) 16: 160–164.

Thomas, O. 1898. On the mammals collected by Mr. John Whitehead during his recent expedition to the Philippines. Transactions of the Zoological Society of London 14: 377–414.

Yoder, A.D., M. Cartmill, M. Ruvolo, K. Smith, and R. Vilgalys. 1996. Ancient single origin for Malagasy primates. Proceedings of the National Academy of Sciences of the United States of America 93: 5122–5126.

Zwickl, D.J. 2006. Genetic algorithm approaches for the phylogenetic analysis of large biological sequence datasets under the maximum likelihood criterion. Ph.D. dissertation, University of Texas at Austin.